Chapter 6 A New Rational Numerical Simulation Procedure for Liquid Cargo Ship Collision

6.1 Introduction

In Chapter 5, only the fluid-structure interaction of liquid cargo tank is taken into account accurately and the surrounding water is simply modelled as rigid point masses along the wetted area in FE model. In order to predict the structural damaged behaviour and the motion of striking/struck motion during ship collision accurately, the effect of surrounding water on ship collision process should be taken into account.

In section 6.2, the accuracy of motion simulation using ALE FE method is validated by sway motion of hull experiment (Motora et al 1969). In section 6.3, numerical simulation procedure of the ship collision between a 350,000 tonne laden VLCC and a 293,000 tonne double hull crude oil carrier, which takes account of both fluid-structure interaction in liquid tank and surrounding water, is presented. In order to understand the structural damage behaviour better, the impact force, absorbed energy, the motion of striking/struck ship and the critical striking velocity are compared.

6.2 Validation of ALE FEM on Sway Motion of Hull Experiment

To check the accuracy of ALE method outlined above for the fluid-structure interaction between the hull and surrounding water, two-dimensional analysis of sway motion of hull experiment (Motora 1969) is carried out. The comparison of computational result and the experimental result is presented.

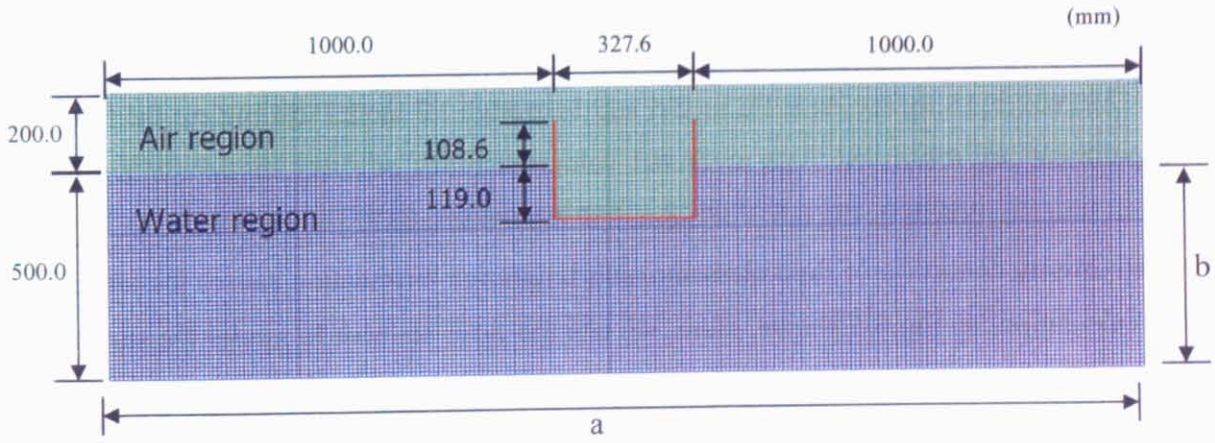

Fig. 6.1 ALE FE model for sway motion experiment

Figure 6.1 shows ALE FE model of sway motion of hull experiment. Since total mass of ship model is $53\,kg$ and the length is $2\,m$, the mass of hull with $\Delta l = 0.01m$ in FEM model is $0.265\,kg$ and the hull is modeled as 75 rigid shell elements. The applied force F in x direction is $0.098\,N$ and the duration time is $0.6\,\mathrm{sec}ond$. In ALE model, the water and air region were modeled as 16310 eight-node solid elements with the mesh size $10mm * 10mm * 10mm$. The dynamic viscosity and bulk modulus of water are $1.0038 \times 10^{-6} m^2/s$ and $2.2 \times 10^9\ N/m^2$ respectively.

The numerical results of displacement and velocity for sway motion are in good agreement with the experimental data in Fig. 6.2. Using ALE finite element method to predict the sway motion of hull, good agreement has been observed. The sway motion process of hull model is indicated in Fig. 6.3.

Since the sway motion of hull is affected by different boundary conditions of surrounding water and the CPU time is influenced by the number of ALE formulation elements, it is necessary to investigate the effect of boundary condition and the range of surrounding water on the sway motion. Three different boundary condition and range of surrounding water were modelled. The velocity curves of sway motion for three different FE model are shown in Fig. 6.4. Table 6.1 indicates the details of the three models and the run time properties.

From the results of Fig.6.4 and Table 6.1, it is found that when the range of surrounding water is modelled as about two times of the dimension of ship hull and the boundary condition set free, the effect of surrounding water can be taken into account well and this FE model is appropriate for predicting the motion of ship in surrounding water with reasonable accurateness and relatively low CPU time required.

Moreover, using the ALE FE model and Lagrange FE model to simulate the hull sway experiment are discussed. The predicted velocity curves of sway motion with different mesh size are plotted in Fig.6.5. For numerical results to converge, fine mesh size should be used. Strong distortion of fluid element using langrange formulation causes the termination of calculation, as Fig.6.5 shown. Here, we use the ALE element to model the surrounding water.

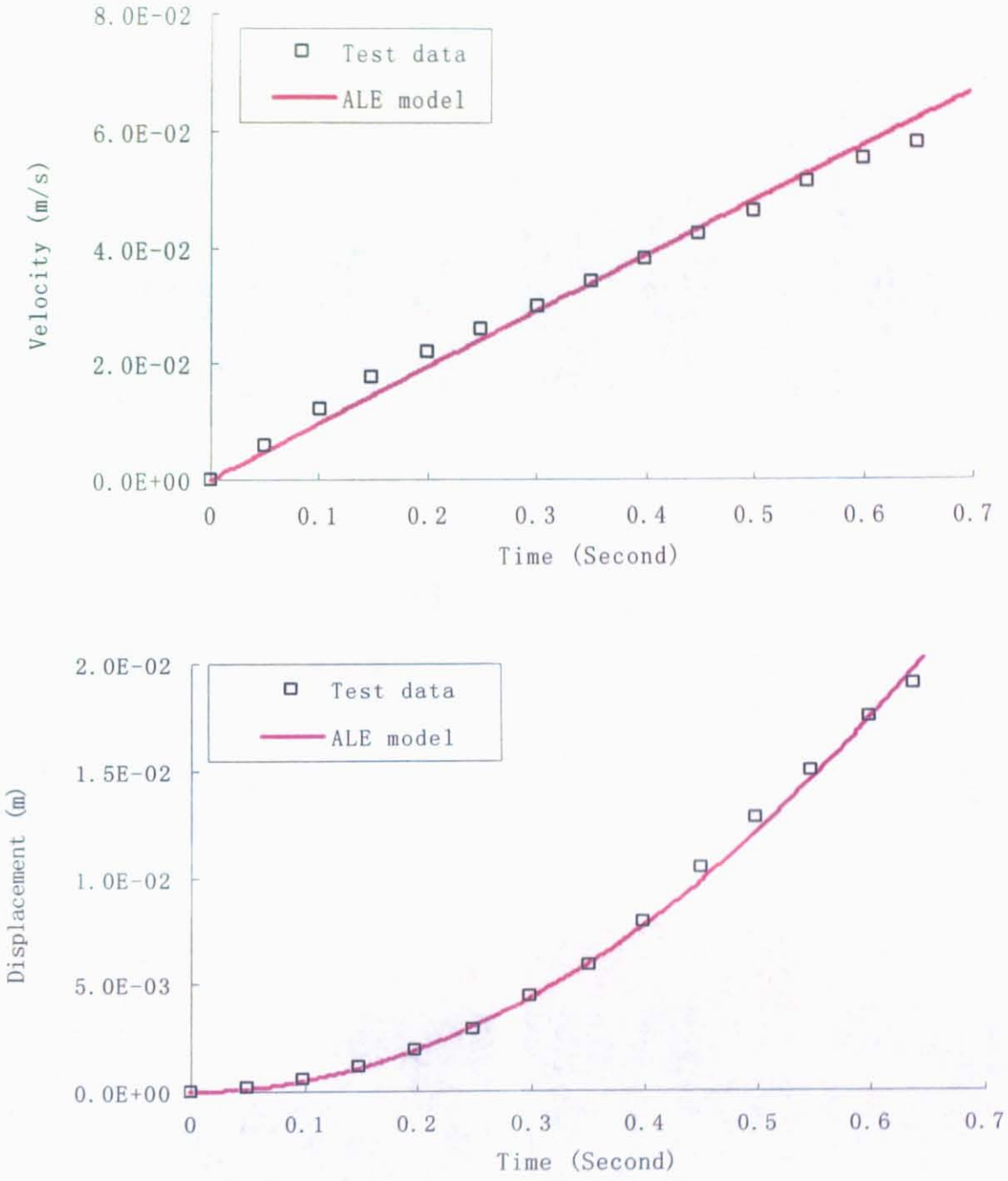

Fig. 6.2 Velocity and displacement of hull for sway motion

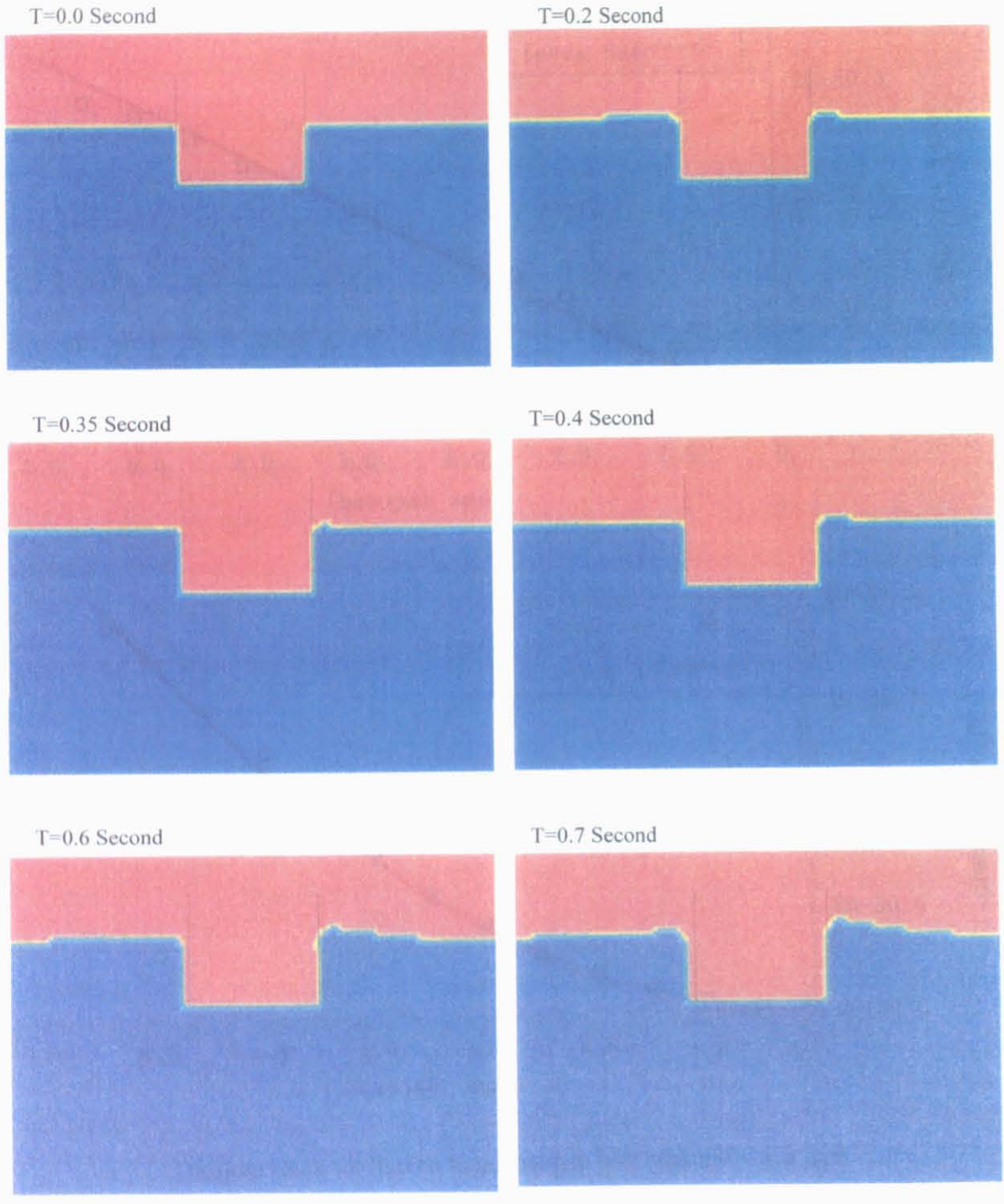

Fig. 6.3 Sway motion of hull at different time

Fig. 6.4 Velocity curve of sway motion for three different FE model

Table 6.1 Details of the three models and the run time properties

	Model 1	Model 2	Model 3
a / B	91.2	4.30	2.87
b / D	16.8	2.69	2.02
Boundary Condition	The same as test	No-reflecting boundary	No-reflecting boundary
Number of ALE Elements	35200	5500	2914
CPU Time (Second)	1986	307	177

where

a the breadth of surrounding water

b the depth of surrounding water

B the breadth of hull model

D the draught of hull model

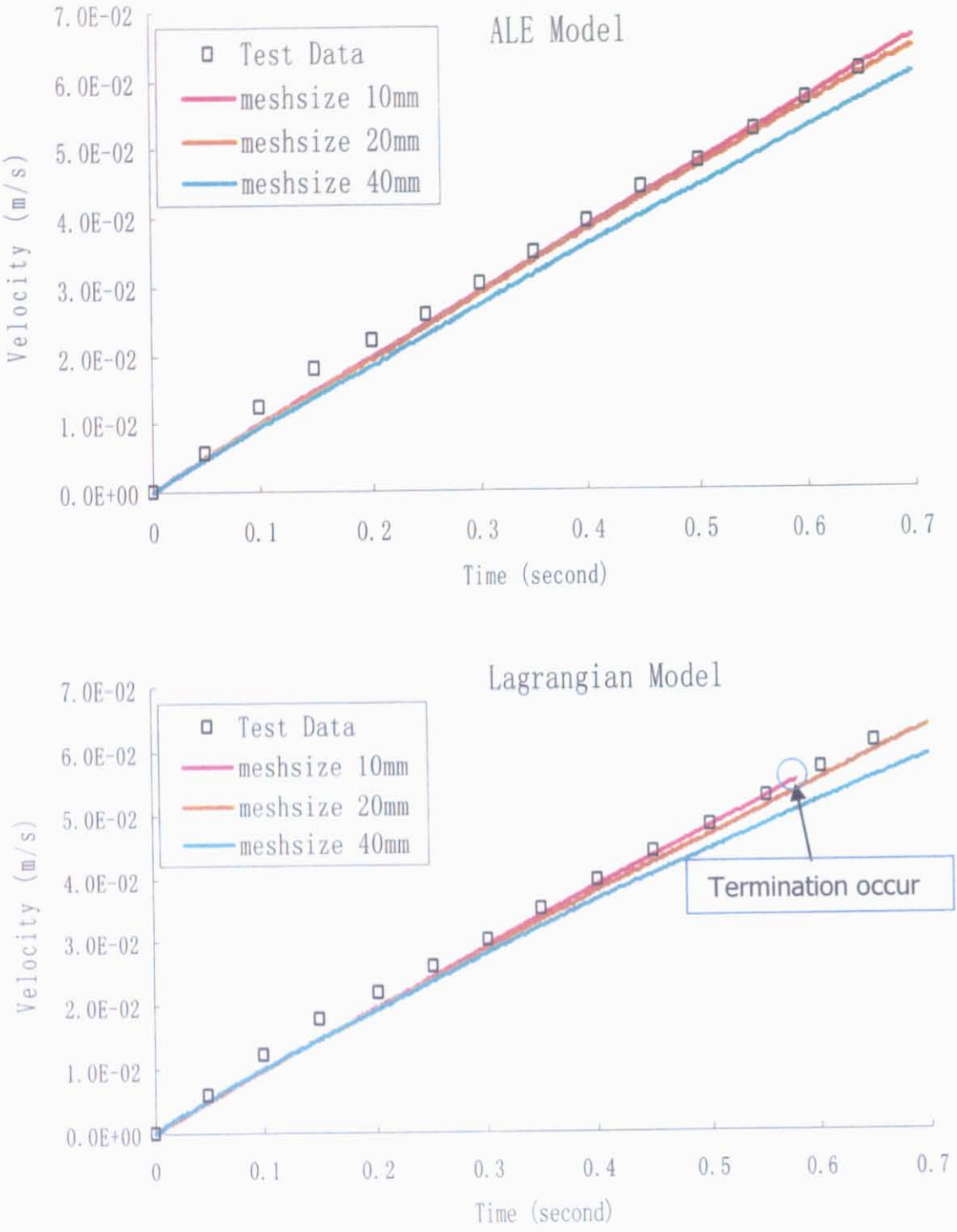

Fig. 6.5 Velocity curve of sway motion for different element formulation

6.3 Ship Collision of Double Hull Oil Tanker

6.3.1 General Description

In chapter 5, the numerical simulation of ship collision only the fluid-structure interaction of liquid cargo tank is taken into account accurately and the surrounding water is simply modelled as rigid point masses along the wetted area in FE model. In this chapter, numerical simulation of ship collision, taking fluid-structure interaction of both surrounding water and liquid cargo tank into account, will be carried out.

The principal dimensions of the struck ship, collision scenario and load condition of VLCC are the same as those of the model in chapter 5. The principal dimensions of the striking ship and the struck ship are shown in Table 6.2. All structural members in the struck ship were also assumed to be made in mild steel, with the material properties given in Table 6.3. The same simplified material model in Section 4.4.4, which uses the equations (4.2)-(4.4) to set up true stress-strain curve, was used in numerical simulation.

Table 6.2 Principal dimensions of the striking ship and the struck ship

Parameter	The Striking Ship (350,000 tonne VLCC)	The Struck Ship (293,000 tonne VLCC)
Length (m)	330.0	327.0
Breadth (m)	58.0	56.4
Depth (m)	32.5	30.6
Draught (m)	21.0	19.8

Table 6.3 Material property for struck ship model

Thickness (mm)	Yield Strength (MPa)	Ultimate Strength (MPa)	Experimental Rupture Strain	Young's Modulus (MPa)	Poisson Ratio
20	329	420	0.402	2.06×10^5	0.3

6.3.2 Crude Oil Modeling

According to the conclusion of chapter 5, modelling the crude oil as solid elements with Lagrangian formulation is appropriate for predicting the fluid-structure interaction of liquid cargo tank during ship collision, as well as with a relatively low CPU time. In this chapter, the crude oil in liquid tank is modelled as 66700 solid elements with $1.5m * 1.0m * 1.0m$.

6.3.3 Surrounding Water Modeling

There are two different numerical models to consider the effect of surrounding water in ship collision, namely Added Mass model and Arbitrary Lagrangian Eulerian model.

In most previous literature, the added mass distribution due to the movement of the struck ship in the surrounding is modelled as point masses along the wetted area in FE model.

To improve the accuracy, the surrounding water can be modelled as ALE formulation elements taking the effect of surrounding water into consideration. Based on the principal dimension of stuck ship, the surrounding water is modelled as 104880 ALE elements with $4.7m * 1.8m * 2.5m$ in Fig. 6.6. The range of surrounding water is $380\,m$ in length, $140\,m$ in breadth and $41.5\,m$ in height.

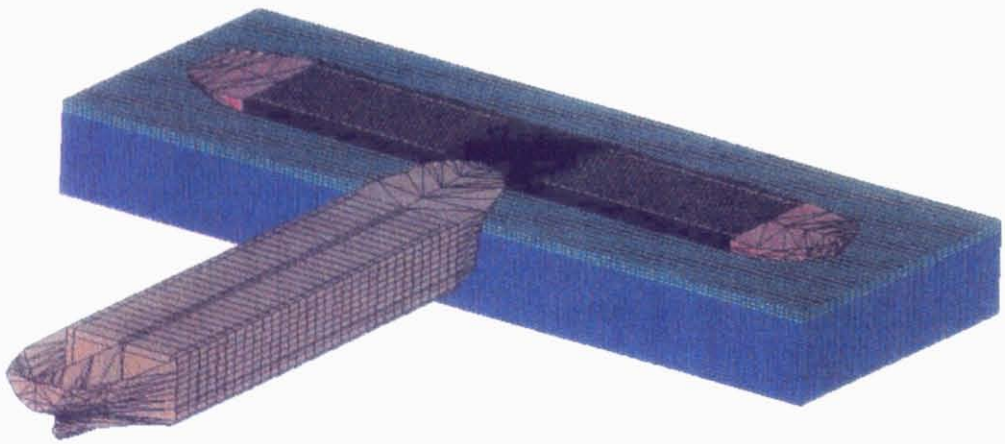

Fig. 6.6 ALE model of ship-ship collision including surrounding water

6.4 Analysis of Results

The absorbed internal energy, the impact force between the bow and struck ship, motions of striking/struck ship and critical striking velocity for different numerical models obtained from the simulations were compared.

The damage process of struck ship at different time using ALE FE model and Added Mass Model are shown in Fig.6.7 and 6.8. Figure 6.9 and 6.10 show the progressive damage process of struck cargo tank at different time in ALE FE model and Added Mass model respectively. When reviewing the progressive damage process for 2 different models, the difference of the structural damage extent between ALE Model and Added Mass Models is quite small at time of outer shell structure rupture. This means that Added Mass Models can consider the effect of surrounding water well in initial phase. The time of inner shell rupture in ALE FE model is 0.976 second, which is much later than that of Added Mass model. At collision time 1.0 second, the damage extent of side structure in ALE Model is less than that of Added Mass Model.

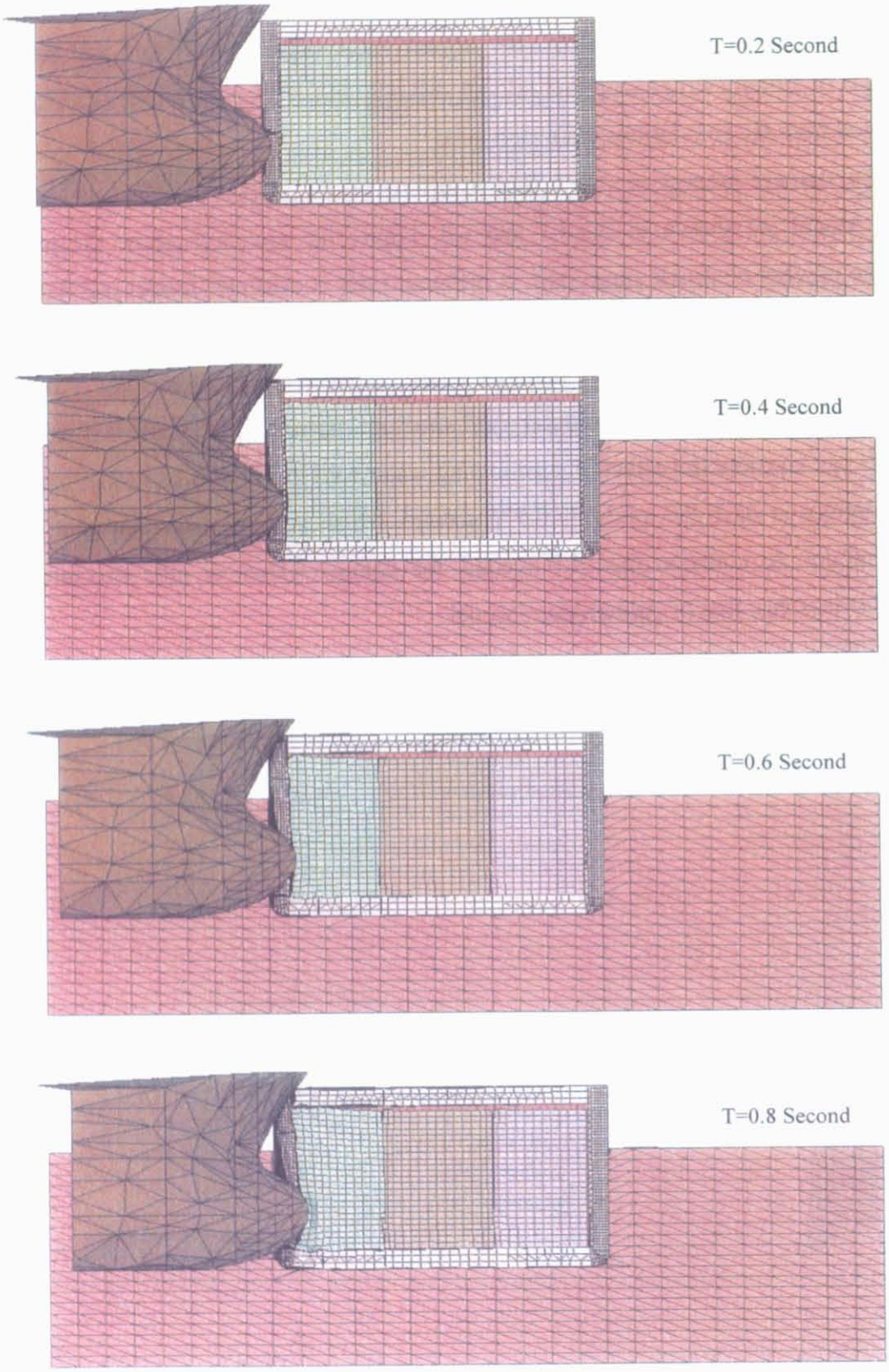

Fig. 6.7 Deformation of struck ship at different time for ALE FE Model

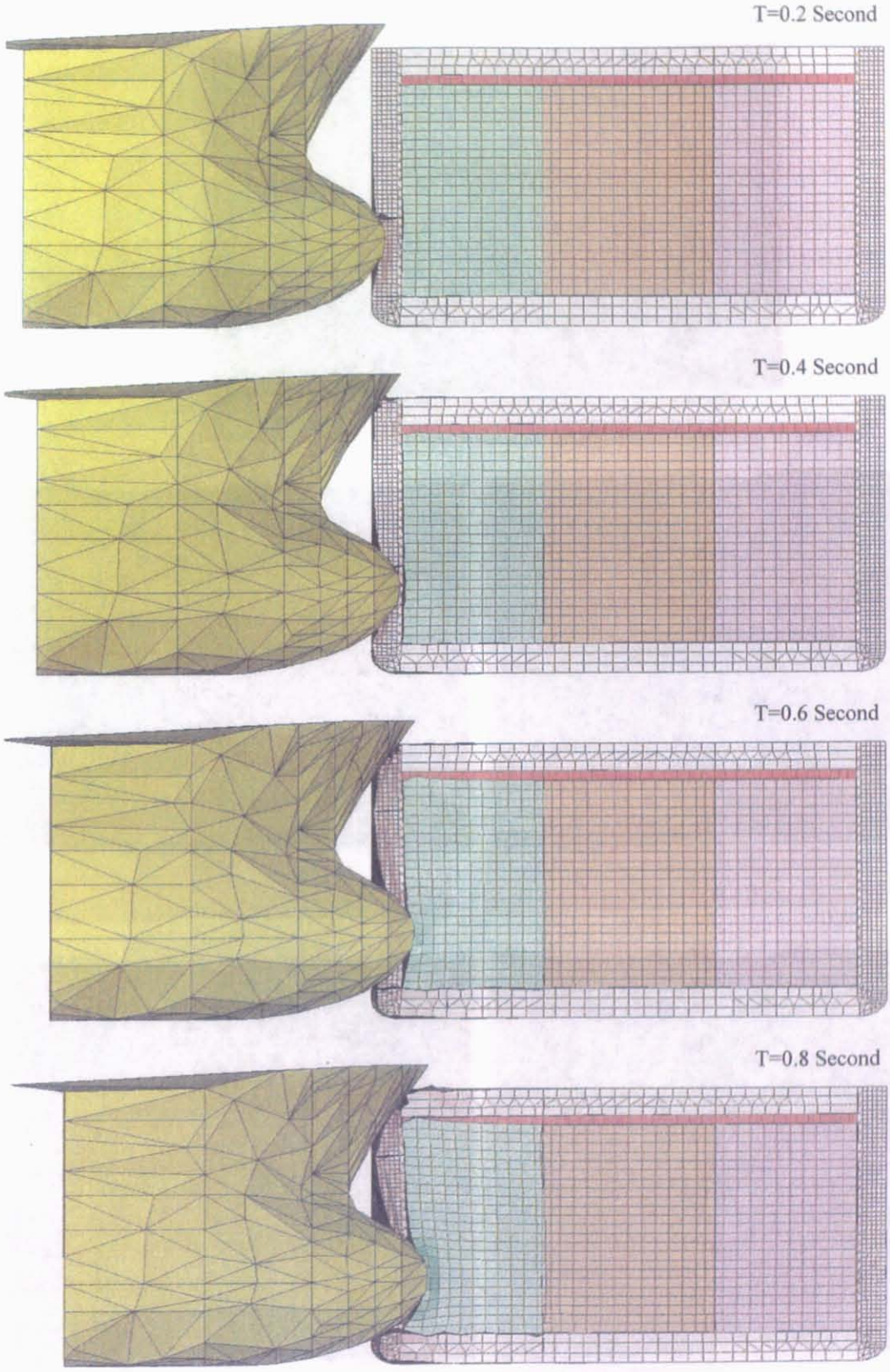

Fig. 6.8 Deformation of struck ship at different time for Added Mass Model

Rupture of outer shell T=0.272 s

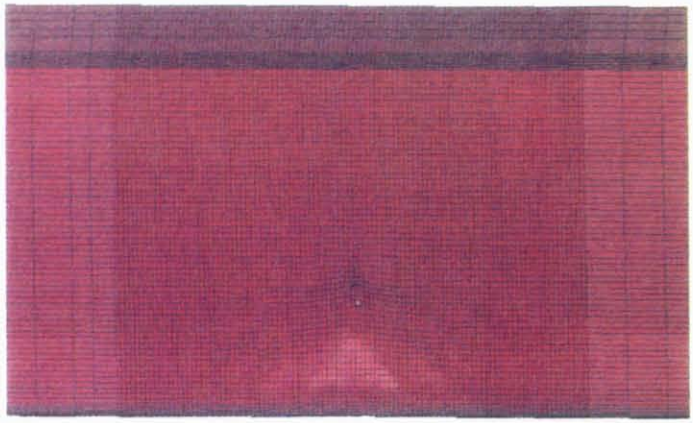

Rupture of inner shell T=0.976 s

T=1.0 s

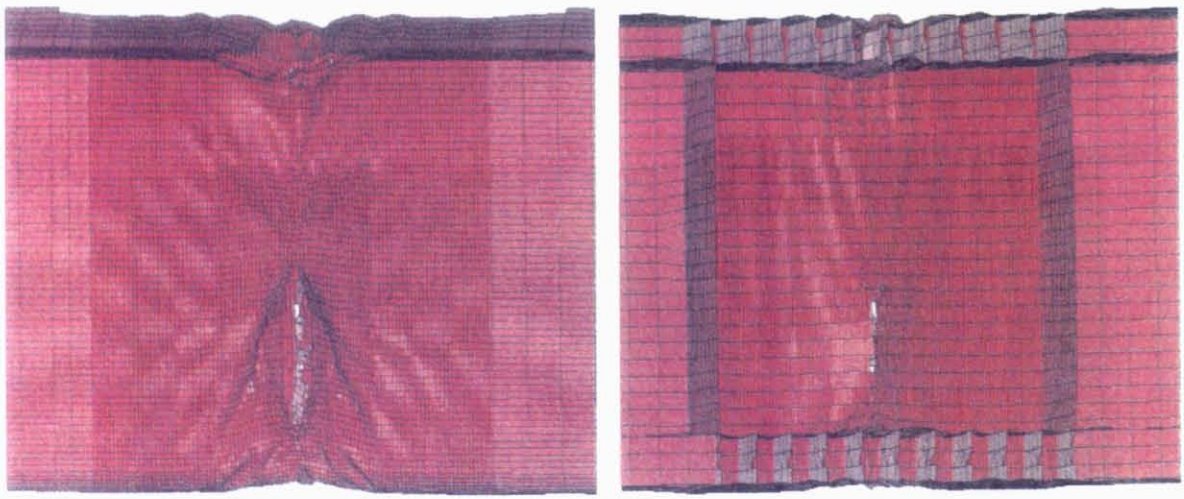

Fig. 6.9 Damaged tank at different time in ALE FE model

Rupture of outer shell T=0.266 s

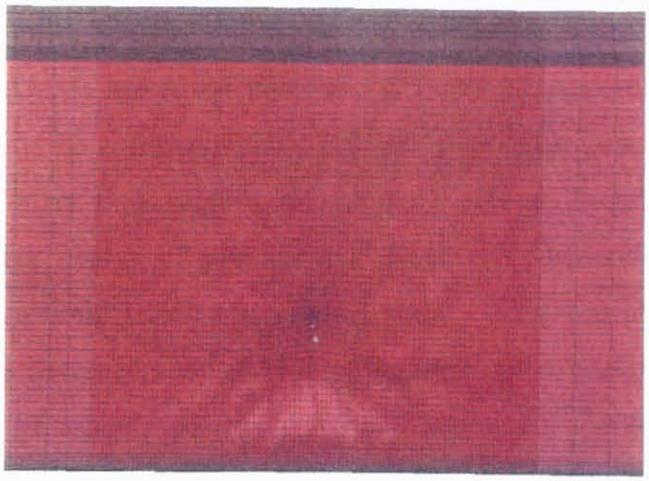

Rupture of inner shell T=0.736 s

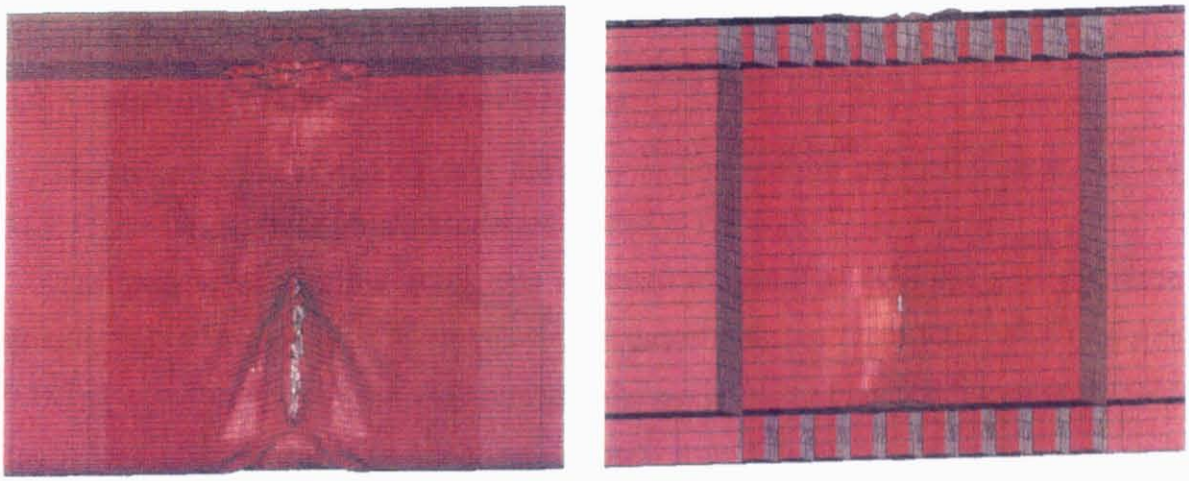

T=1.0 s

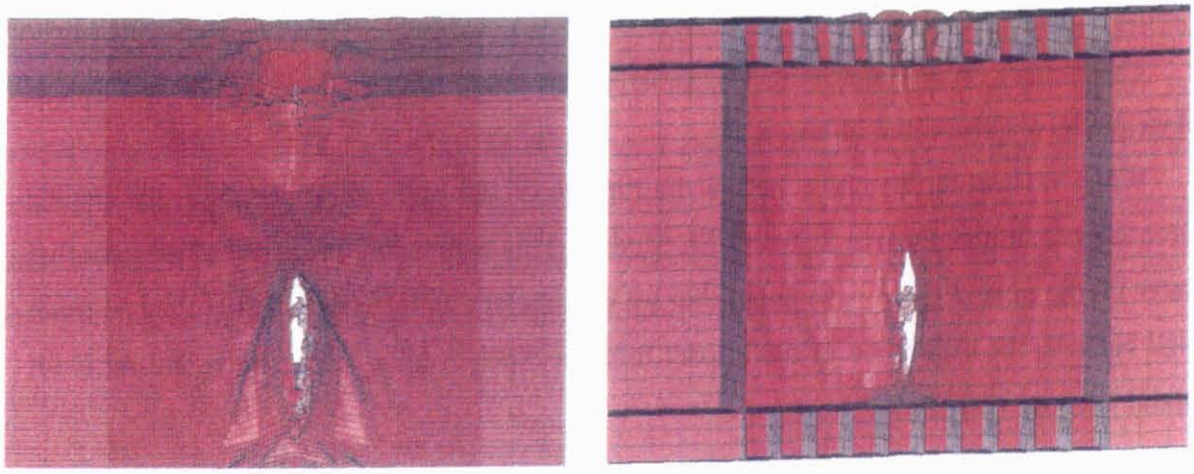

Fig. 6.10 Damaged tank at different time in Added Mass model

6.4.1 The Impact Force-penetration Curves

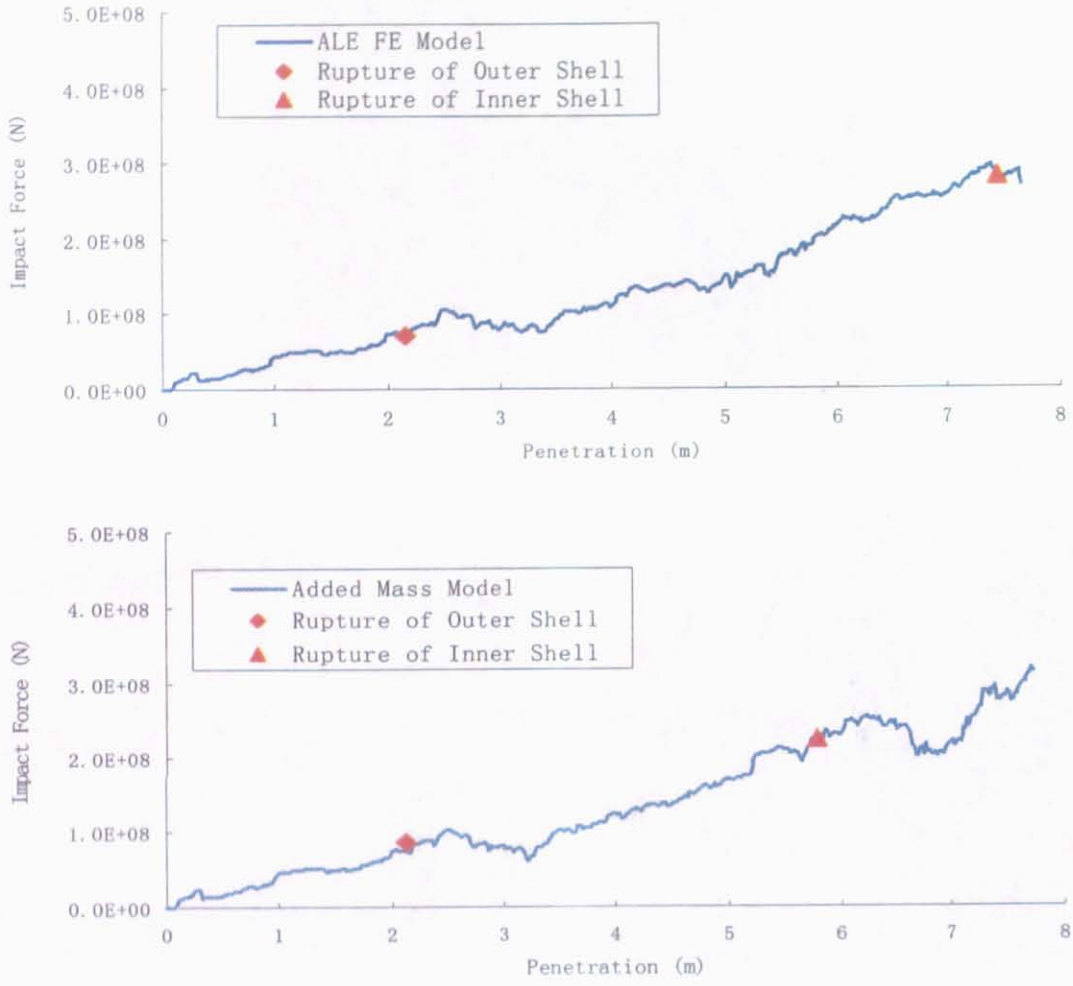

Fig. 6.11 Impact force-penetration curves for different FE Models

The impact force-penetration curves of struck cargo tank in ALE model and Added Mass model are presented in Fig. 6.11.

When reviewing the plots, before the rupture of the outer shell occurred, the impact force is very similar for two different FE Models. This means that the effect of surrounding water on the impact force is so small that we can neglect its influence. At the time of inner shell rupture, the difference of the impact force between Added Mass Model and ALE FE model is about 19.72%.

6.4.2 Energy Balance Results

Here the kinetic energy of striking/struck ship, internal energy of struck ship for ALE FE model and Added Mass Model are presented in Fig. 6.12. According to the plots, most of dissipated energy in the collision simulation was absorbed by internal energy of struck ship. At the time of inner shell rupture, only about 1.27% of the total initial energy was absorbed by the kinetic energy of struck ship (92 MJ) and surrounding water (30 MJ) in ALE FE model, whereas in Added Mass model about 0.2% was absorbed. The internal energy of struck ship absorbed about 8.43% of the total initial energy at the time of inner shell rupture in ALE FE model, whereas in Added Mass model about 5.48% was absorbed. The Added Mass Model is overestimate 34.99% absorbed energy of struck ship compared with the results of ALE FE model at the point of inner shell rupture.

6.4.3 Motions of Striking/Struck Ships

The surge motion of striking ship, the sway motion and roll motion of struck ship for ALE FE model and Added Mass Model are plotted in Fig. 6.13.

The sway velocity of the struck ship increased of course as the surge velocity of the striking ship decreased. The sway velocity of the struck ship for Added Mass model is $0.187\,m/s$ at the time of inner shell rupture, whereas in ALE FE model is about $0.329\,m/s$. The Added Mass Model is underestimate 43.16% sway velocity of struck ship compared with the results of ALE FE model at the point of inner shell rupture. The roll velocity of the struck ship for Added Mass model is $3.05\times10^{-3}\ rad/s$ at the time of inner shell rupture, whereas in ALE FE model is about $2.86\times10^{-2}\ rad/s$. The Added Mass Model is underestimate 89.34% roll velocity of struck ship compared with the results of ALE FE model at the point of inner shell rupture. Obviously, there is the necessary to introduce ALE model to describe the fluid-structure interaction between the struck ship and surrounding water in order to predict the motion of struck ship accurately.

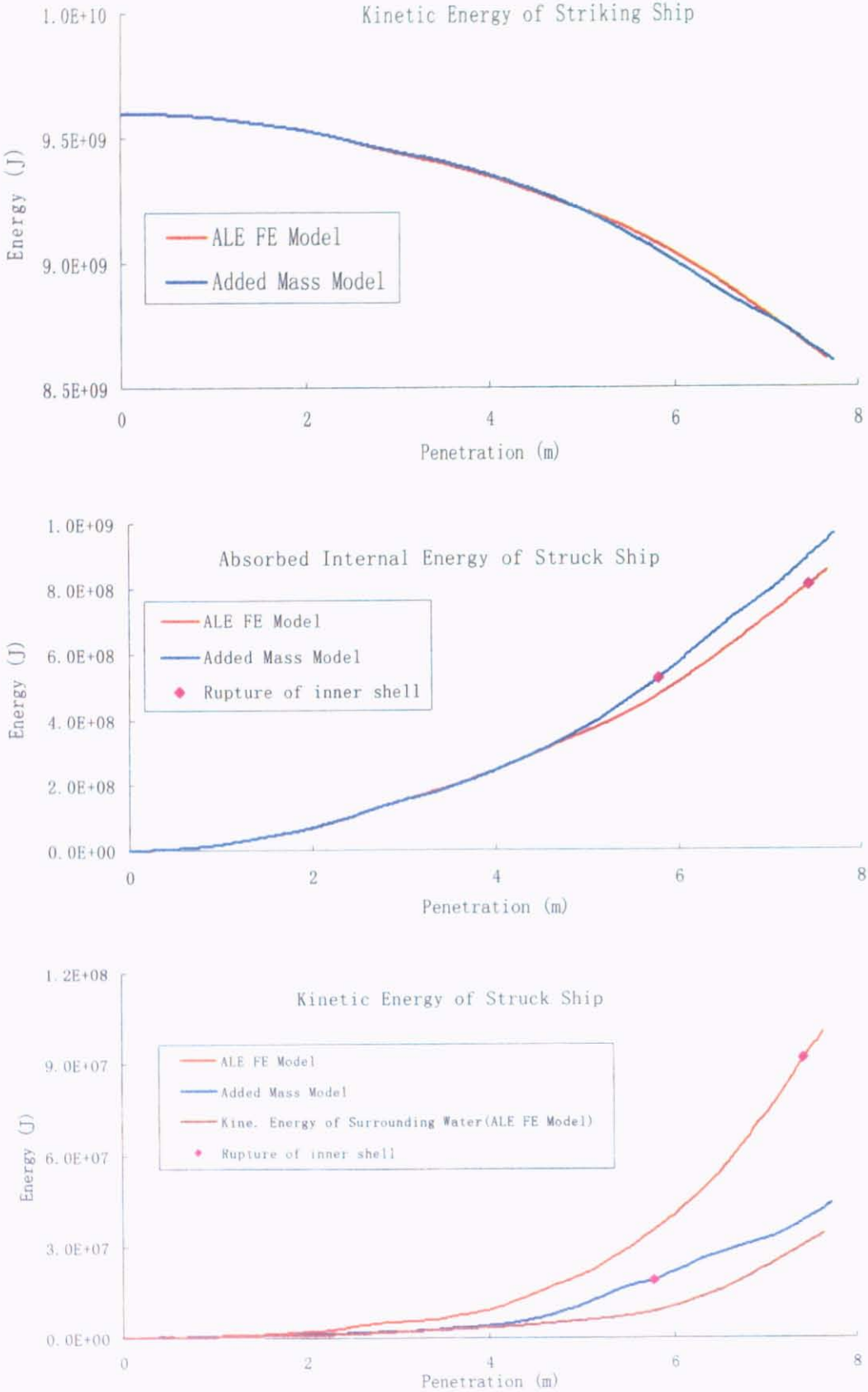

Fig. 6.12 Different energy-time curves of striking/struck ships

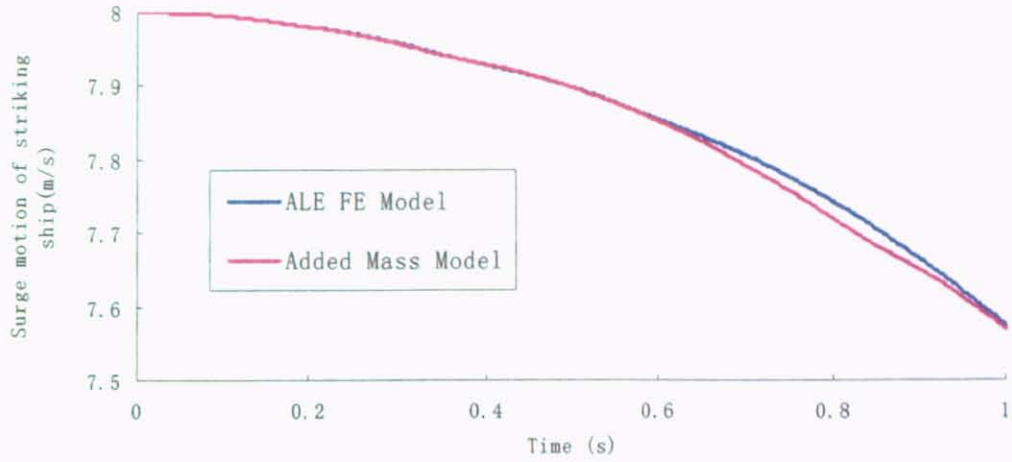

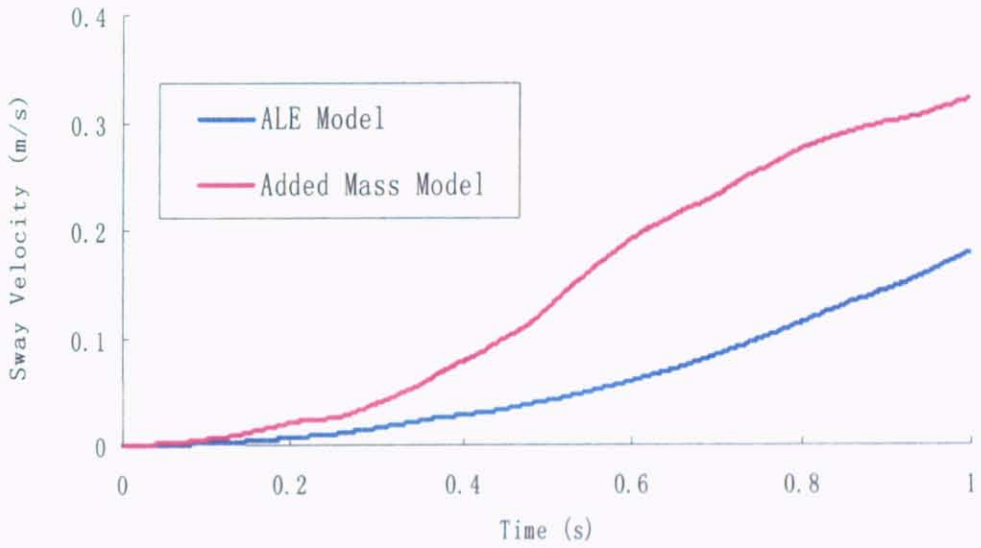

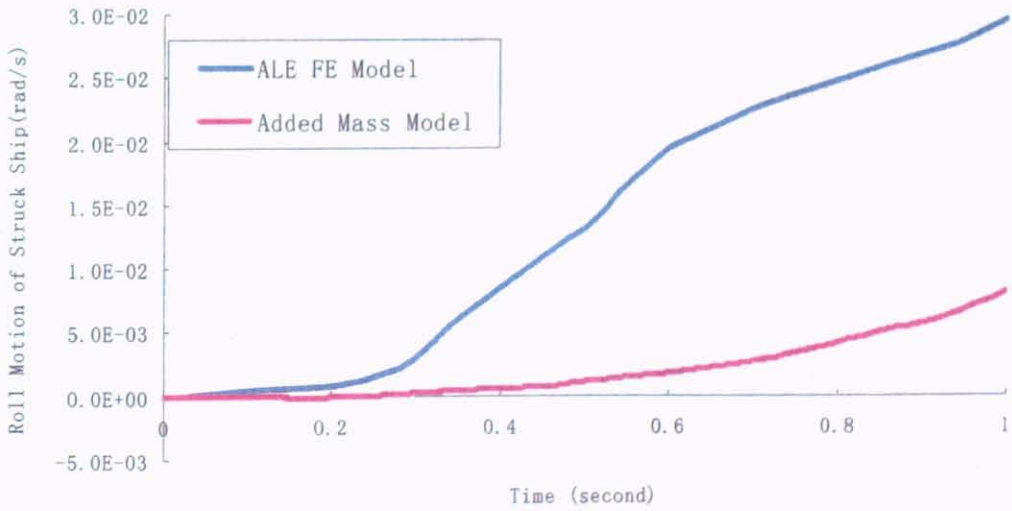

Fig. 6.13 Different motion-time curves of striking/struck ships

6.4.4 Critical Velocity of Striking Ship

Here the critical velocity of striking ship is used to evaluate the crashworthiness of liquid cargo tanker (VLCC) structures

The critical velocity of striking ship is defined as the minimum initial striking velocity, where the striking ship and struck ship will have the same velocity when the rupture of inner shell happened (Endo 2004)

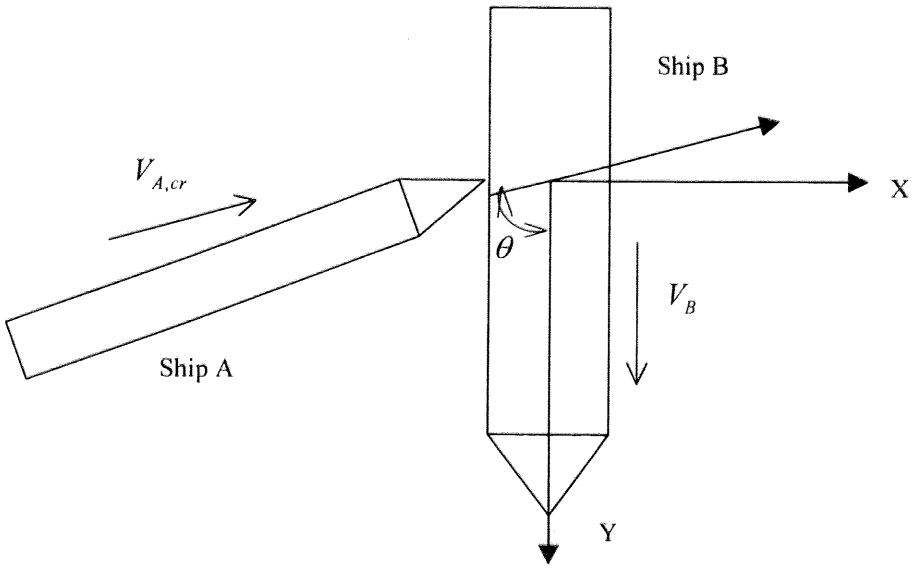

Fig. 6.14 Coordinate system for ship-ship collision

When the striking ship A, which sails at critical velocity $V_{A,cr}$ with collision angle θ, collides with struck ship sailing at V_B, as Fig.6.14 shown.

We assume that the conservation of energy and momentum is satisfied during collision, the equations can be written

$$\frac{1}{2}M_A V_{A,cr}^2 + \frac{1}{2}M_B V_B^2 = \frac{1}{2}(M_A + M_B)V'^2 + E_{S,cr} \tag{6.1}$$

$$M_A V_{A,cr} \sin\theta = (M_A + M_B)V' \cos\beta \tag{6.2}$$

$$-M_A V_{A,cr} \cos\theta + M_B V_B = (M_A + M_B)V' \sin\beta \tag{6.3}$$

where

M_A / M_B displacement of striking/struck ship including added mass

$V_{A,cr}$ critical velocity of striking ship

V_B initial velocity of struck ship

V' velocity of striking and struck ship when rupture of inner shell happened

$E_{S,cr}$ absorbed critical energy when rupture of inner shell happened

θ collision angle between $V_{A,cr}$ and Y-axes

β angle between V' and X-axes

The equation of $V_{A,cr}$ is given by

$$\frac{M_A \cdot M_B}{M_A + M_B} \cdot V_{A,cr}^2 + \frac{2M_A M_B V_B \cos\theta}{M_A + M_B} \cdot V_{A,cr} + \frac{M_A M_B}{M_A + M_B} V_B^2 - 2E_{S,cr} = 0 \qquad (6.4)$$

To solve the equation of (6.4), we can get the critical velocity of striking ship.

For the ship-ship collision case in this chapter, $V_B = 0$ and $\theta = 90°$, then

$$V_{A,cr} = \sqrt{2E_{S,cr} \times \frac{M_A + M_B}{M_A M_B}} \qquad (6.5)$$

In table 6.2, the penetration depths, impact forces, energy results, motion results and critical striking velocities at the point of inner shell rupture for three different FE models are given.

Table 6.4 Simulation results at penetration of the inner side shell

	ALE FE Model	Added Mass Model
Time of inner shell rupture(s)	0.972	0.736
Penetration depth (m)	7.45	5.79
The impact force (MN)	280	225
Kinetic energy of striking ship(MJ)	8669	9056
Velocity of Striking ship(m/s)	7.60	7.77
Kinetic energy of surrounding water (MJ)	30.32	-
Kinetic energy of struck ship(MJ)	91.61	18.93
Velocity of struck ship(m/s)	0.79	0.36
Internal energy of struck ship(MJ)	810	526
Critical Striking Velocity (m/s)	3.14	2.53

6.5 Remarks

Through validation of the ALE FE method on sway motion of hull experiment, the ALE FE method is proved to be suitable to simulate the fluid-structure interaction between the surrounding water and hull. Numerical simulation of the ship collision between a 350,000 tonne VLCC in laden condition collide with a 293,000 tonne double hull VLCC, taking account of both fluid-structure interaction in liquid tank and surrounding water, is presented. Compared with the results of ALE FE Model and Added Mass Model, effect of surrounding water on the structural damage process and motion of striking/struck ships is significant. In order to improve the accuracy of structural damage and motions of striking/struck ships, ALE FE model should be used to model surrounding water. Using ALE FE method, a rational procedure for assessing the crashworthiness of liquid products tanker structures, where the effect of liquid cargo in tank and surrounding water is taken into account is proposed:

1) The fluid-structure interaction of oil in tank is modeled as Lagrangian FE method with reasonable accurateness and a relatively low required CPU time.
2) The fluid-structure interaction of surrounding water and hull structure is modeled as ALE FE method.

Chapter 7 Numerical Analysis Examples for Full Scale Liquid Cargo Ship Collision

7.1 Introduction

In most FE simulations of ship-ship collision presented in the literature the struck ship has been at a standstill. However, statistical data has shown that the struck ship has often a forward velocity at the point of contact and the forward velocity of the struck ship will, of course, have an influence on the damage extent. In order to investigate the structural damage behavior and the motion of striking/struck ships accurately, the detailed parameter study is carried out. The effects of the following parameters are considered: the initial striking velocity, struck ship velocity, the mass of the striking ship and collision angle.

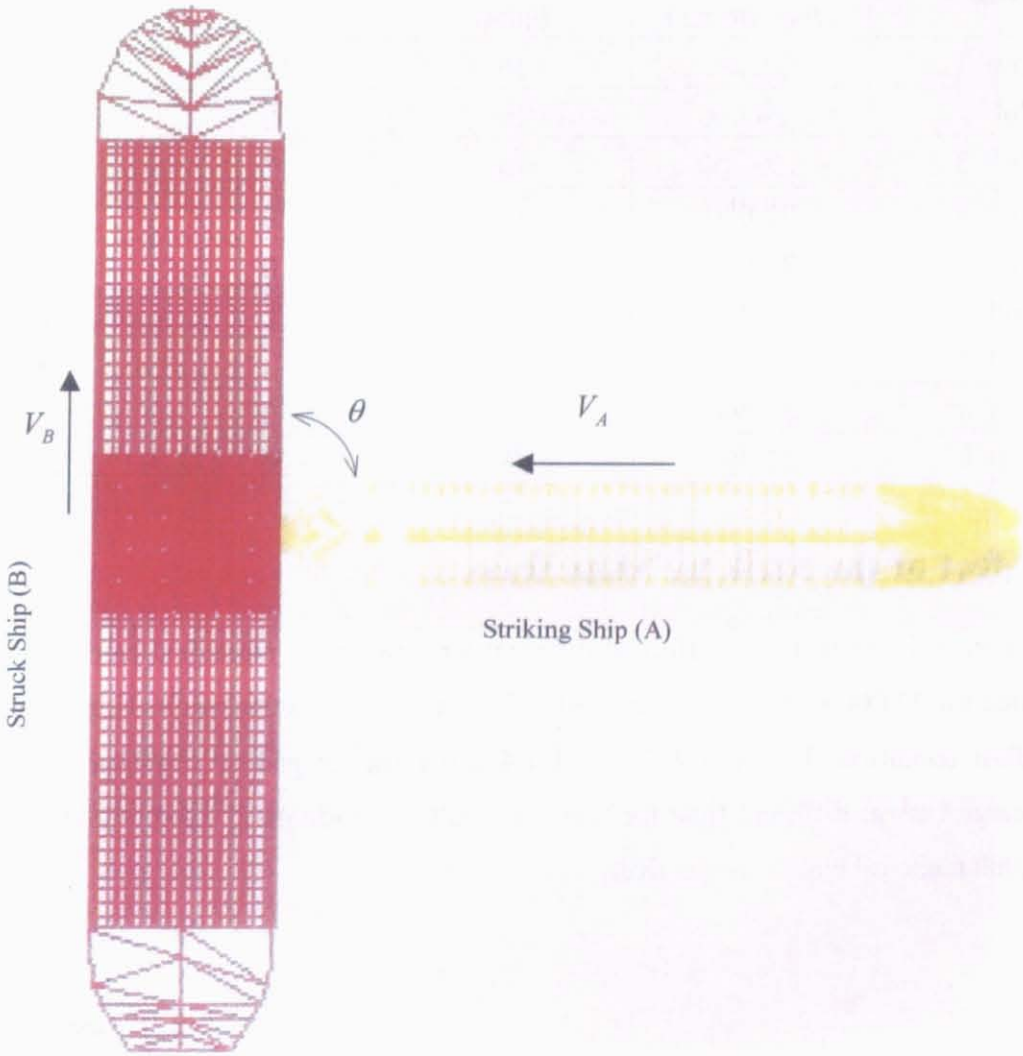

Fig. 7.1 Ship-ship collision model

The principal dimensions and material properties of the striking/struck ships (72,000 tonne oil tanker, 293,000 tonne VLCC and 350,000 tonne VLCC) are the same as those of the model in chapter 5 and chapter 6, which are shown in Table 5.1, 5.2, 6.2 and 6.3. In table 7.1 the different collision scenarios are given. A zero degree collision angle corresponds to a head-on collision and a 90 degree collision therefore corresponds to a perpendicular collision, as Fig. 7.1 shown

Table 7.1 Ship-ship collision scenarios

Collision Scenario	Striking Ship Oil Tanker Disp. (tonne)	Initial Striking Ship Velocity (knot)	Initial Struck Ship Velocity (knot)	Collision Angle
Coll. 1	72,000	16	0	90
Coll. 2	124,000	16	0	90
Coll. 3	350,000	16	0	90
Coll. 4	72,000	14	0	90
Coll. 5	72,000	12	0	90
Coll. 6	72,000	16	8	90
Coll. 7	72,000	16	16	90
Coll. 8	72,000	16	0	75
Coll. 9	72,000	16	0	60

7.2 Effect of the Striking Ship Mass

In order to investigate the effect of different striking mass, numerical calculations are performed for 72,000 tonne oil tanker, 350,000 tonne VLCC oil tanker for laden condition and ballast condition. Figure 7.2, 7.3 and 7.4 show the progressive damage process of struck cargo tank at different time for laden and ballast condition of 350,000 tonne VLCC and 72,000 tonne oil tanker, respectively.

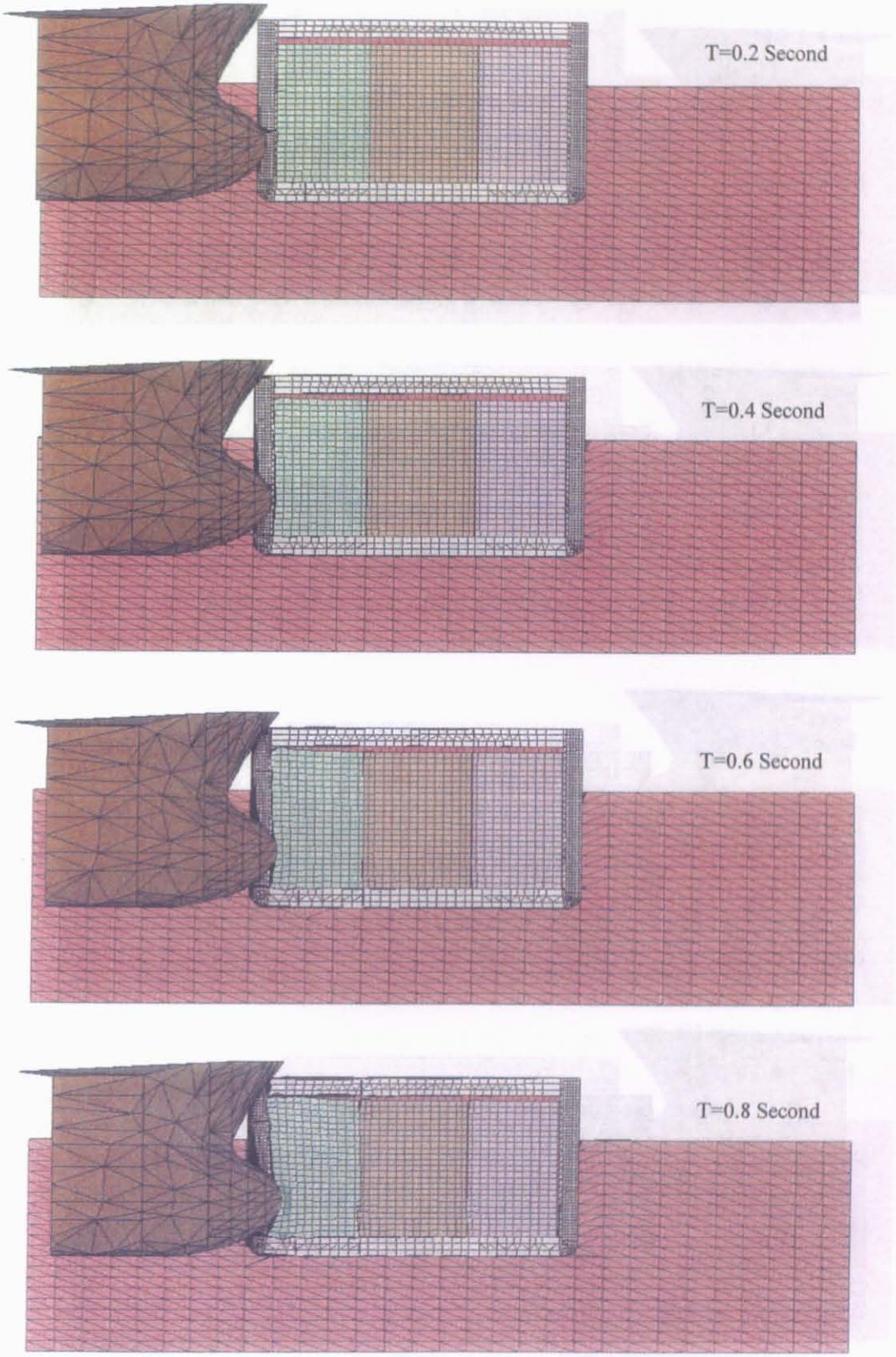

Fig. 7.2 Deformation of struck ship at different time for laden VLCC

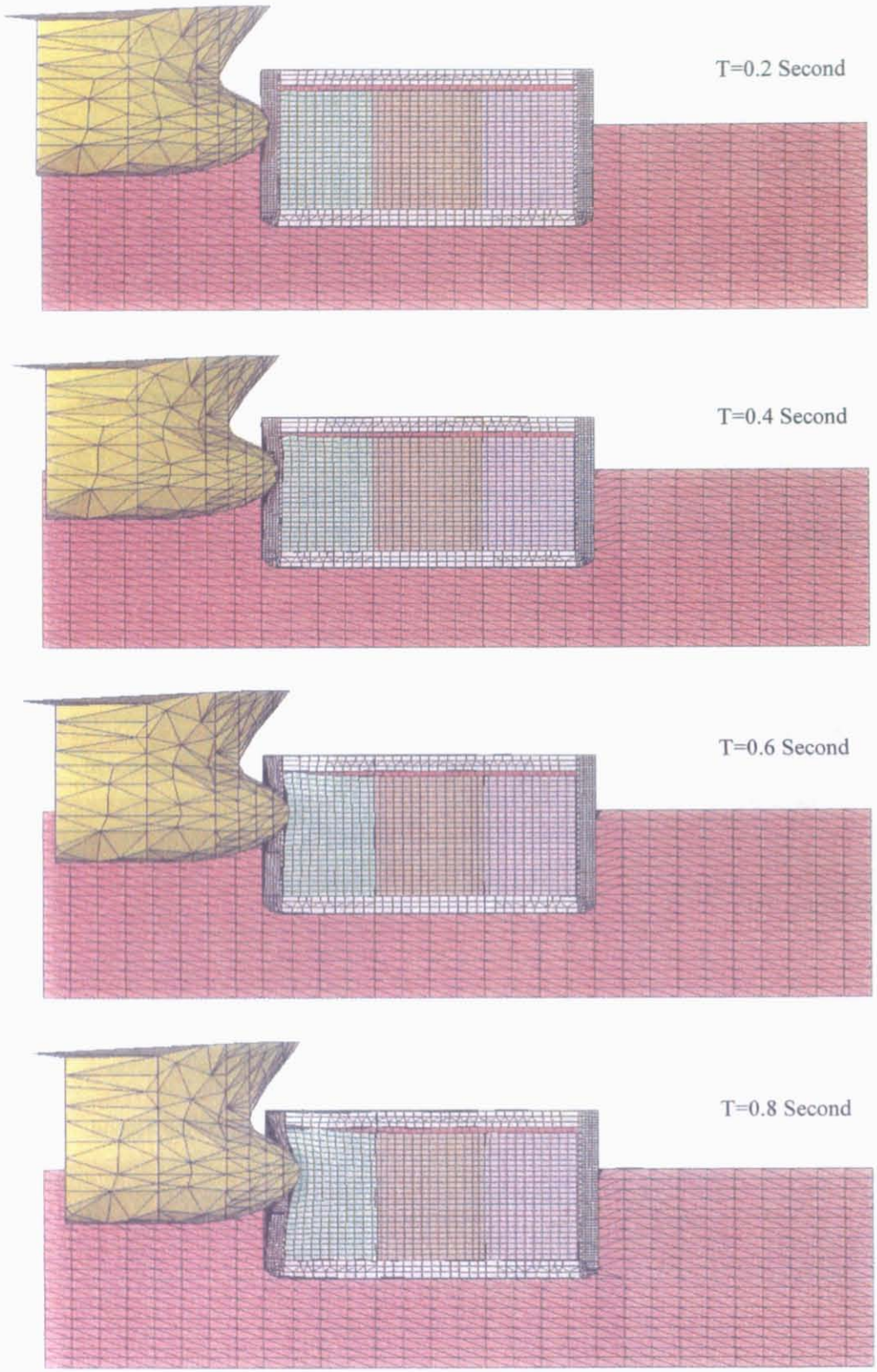

Fig. 7.3 Deformation of struck ship at different time for Ballast VLCC

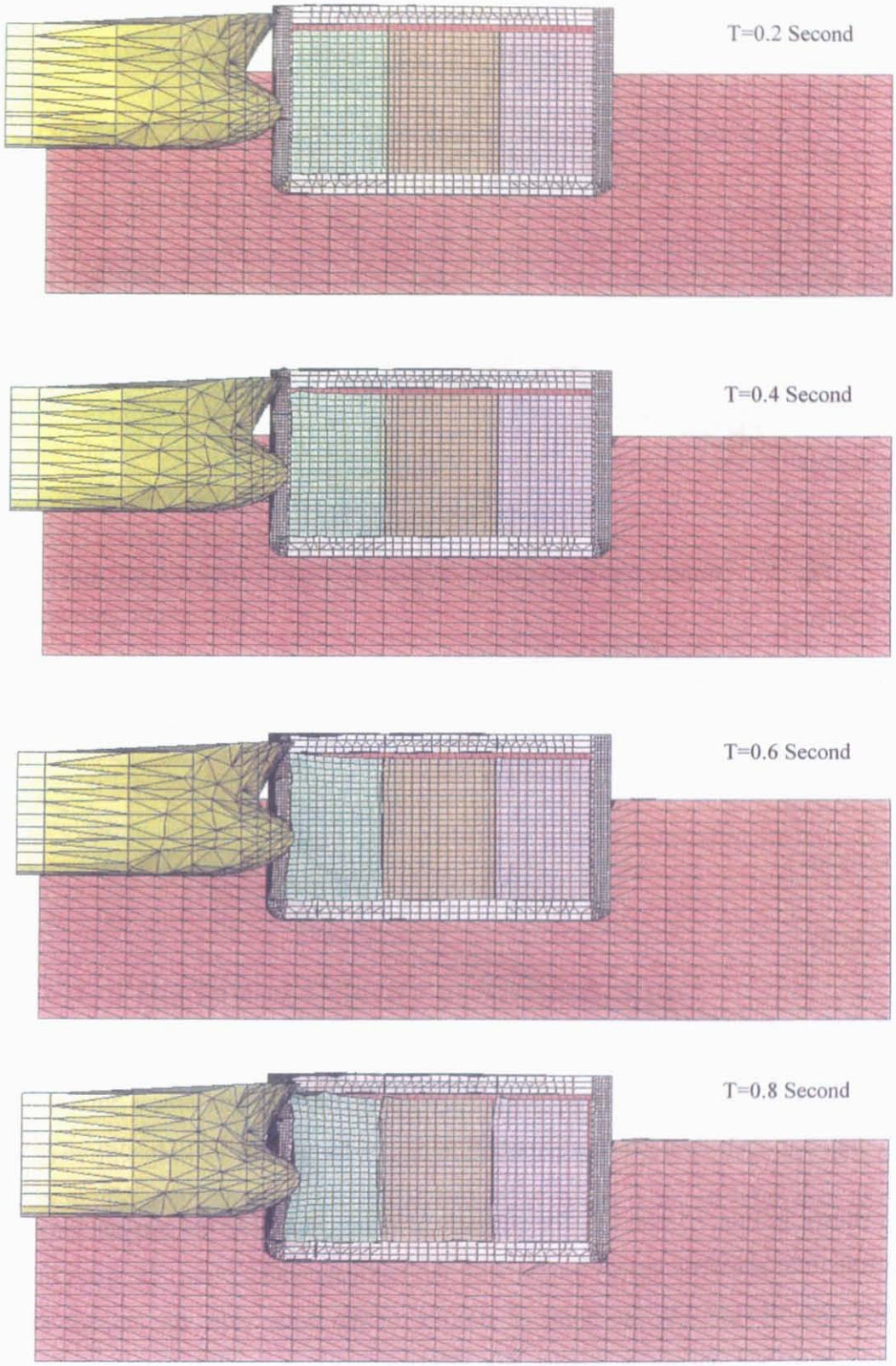

Fig. 7.4 Deformation of struck ship at different time for 72,000 tonne tanker

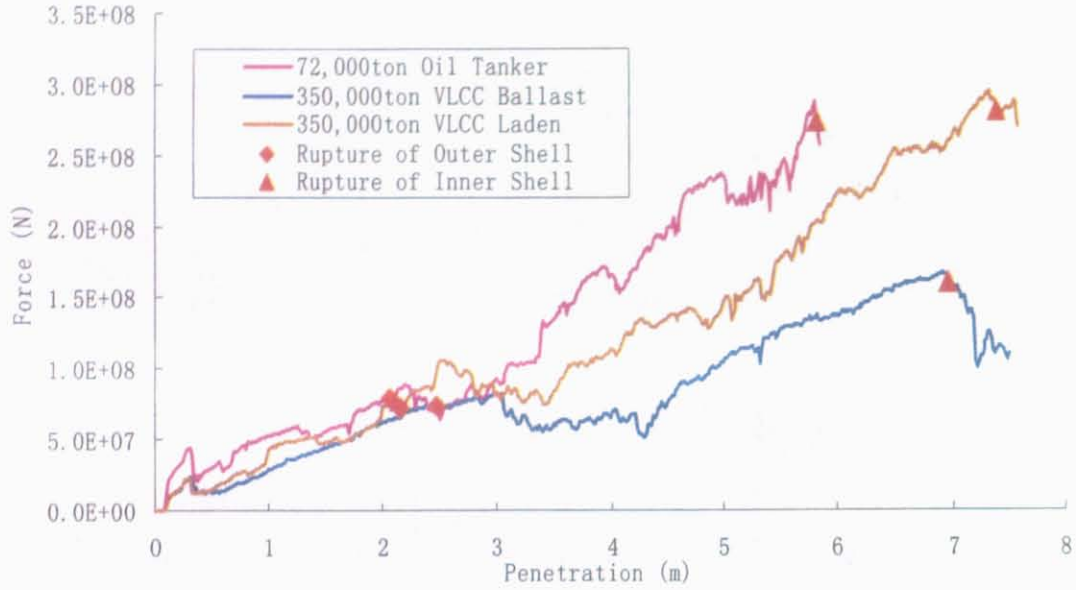

Fig. 7.5 Impact force-penetration curves for various striking ship mass

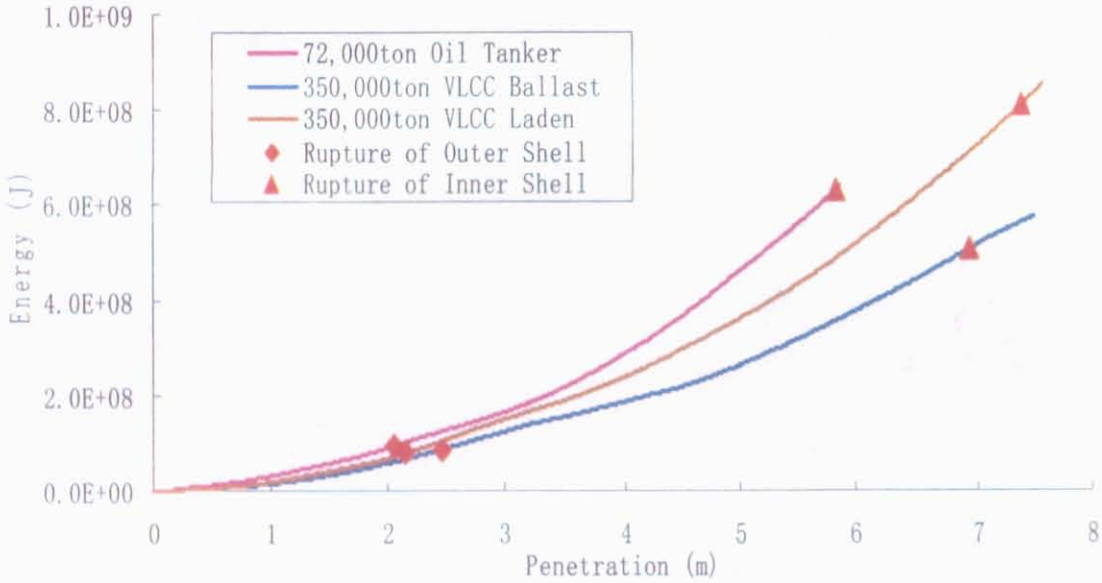

Fig. 7.6 Absorbed energy-penetration curves for various striking ship mass

As shown in Fig. 7.5 and 7.6, for different loading conditions the impact force as well as the structural absorbed energy varied with the vertical contact point, the mass of striking ship and size of bow. At the point of rupture of the outer side, the impact force and structural absorbed energy is similar for different loading conditions. In table 7.2, the penetration depths, impact forces, energy results, motion results and critical striking velocities at the point of inner shell rupture for three different striking ships are given. For

the ballast and laden loading condition, the impact force as well as the structural absorbed energy varied with the contact location at the time of inner shell rupture.

Table 7.2 Simulation results at rupture time of the inner side shell for different striking ship masses

	72,000 tonne Oil Tanker	350,000 tonne VLCC(Ballast)	350,000 tonne VLCC(Laden)
Time of Inner Shell Rupture(s)	0.80	0.916	0.972
Penetration Depth (m)	5.83	5.47	7.38
The Impact Force (MN)	274	161	280
Kinetic Energy of Striking Ship(MJ)	1573	3276	8669
Velocity of Striking Ship(m/s)	6.61	6.95	7.60
Kinetic Energy of Surrounding Water (MJ)	19	9	30
Kinetic energy of Struck Ship(MJ)	82	48	92
Velocity of Struck Ship(m/s)	0.75	0.57	0.79
Internal Energy of Struck Ship(MJ)	630	507	810
Critical Striking Velocity(m/s)	4.40	3.24	3.06

7.3 Effect of the Initial Velocity of Striking Ship

In order to investigate the effect of initial velocity of striking ship on the structural damage behavior, numerical calculations are performed for the initial striking velocity with 16 knot, 14 knot and 12 knot. Figure 7.7 and 7.8 show the progressive damage process of struck ship at different time for the initial striking velocity with 14 knot and 12 knot, respectively

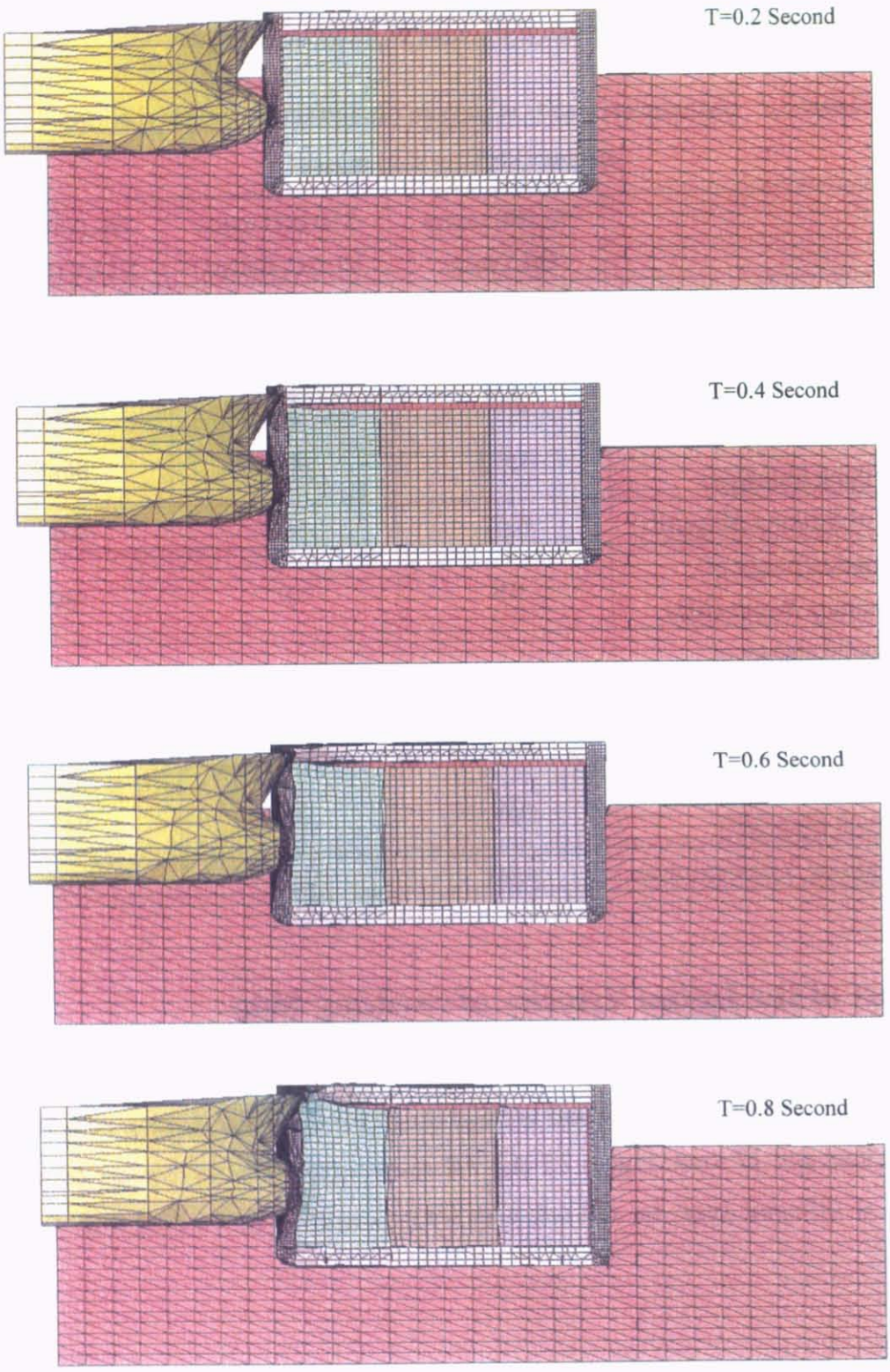

Fig. 7.7 Deformation process of struck ship for 14 knot initial striking velocity

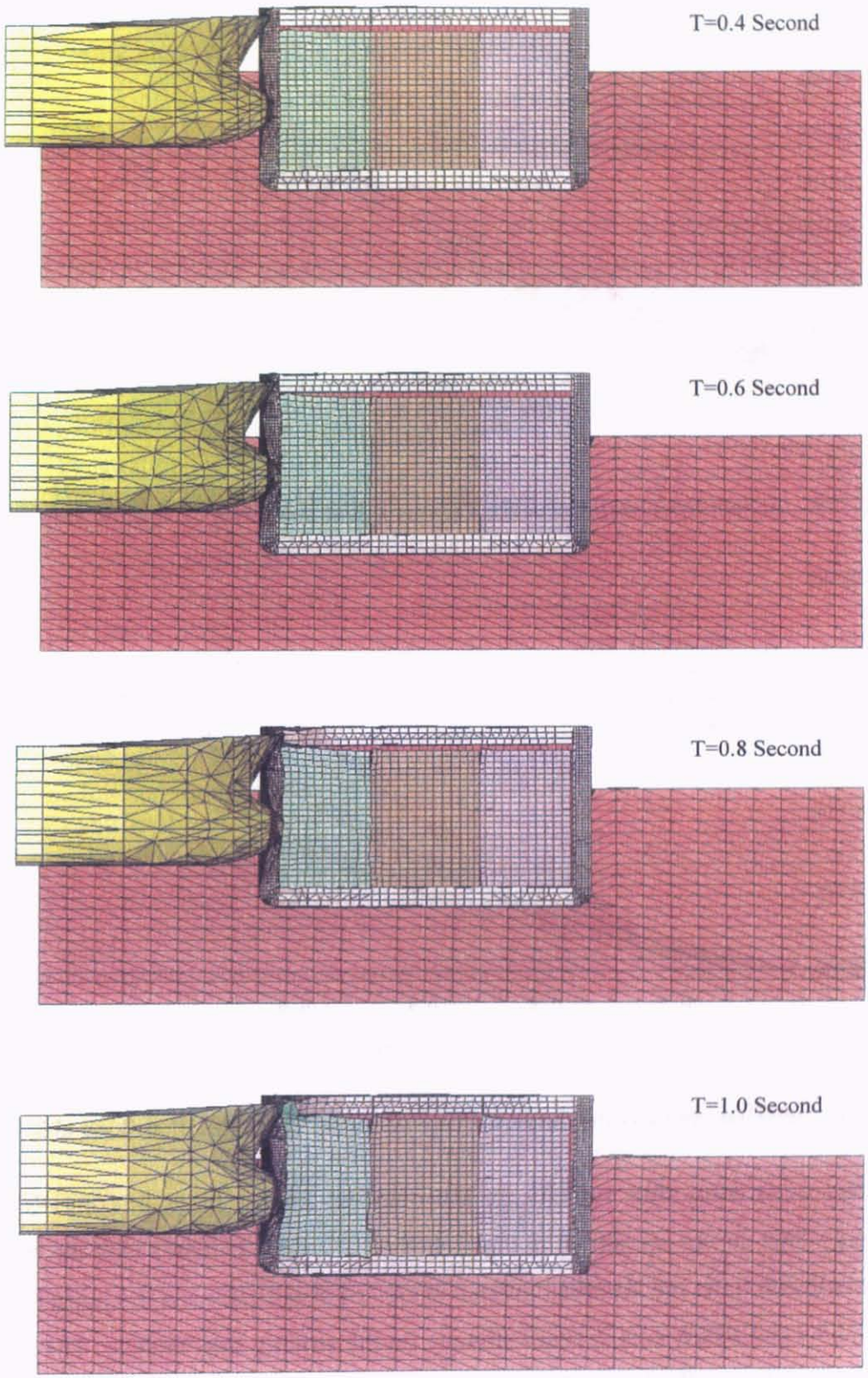

Fig. 7.8 Deformation process of struck ship for 12 knot initial striking velocity

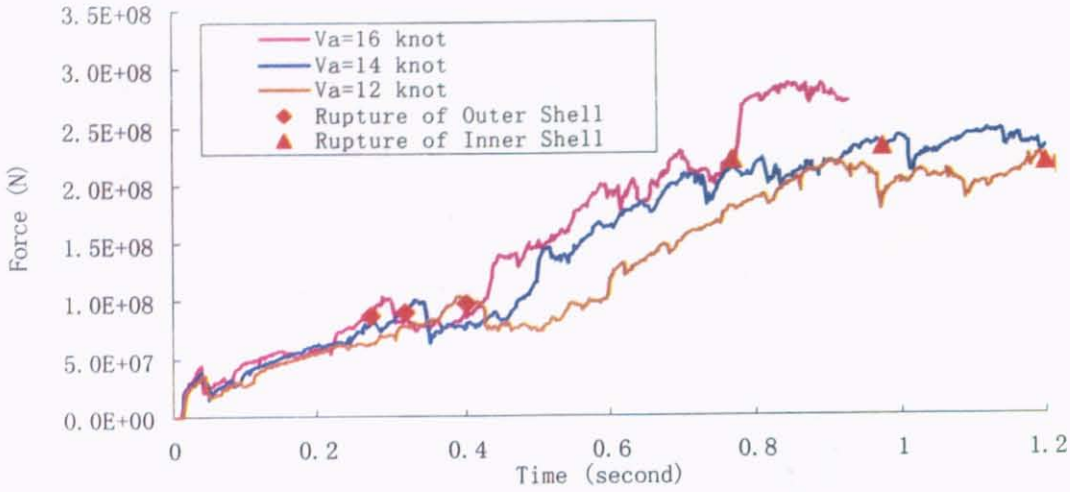

Fig. 7.9 Impact force-time curve for various initial velocities of striking ship

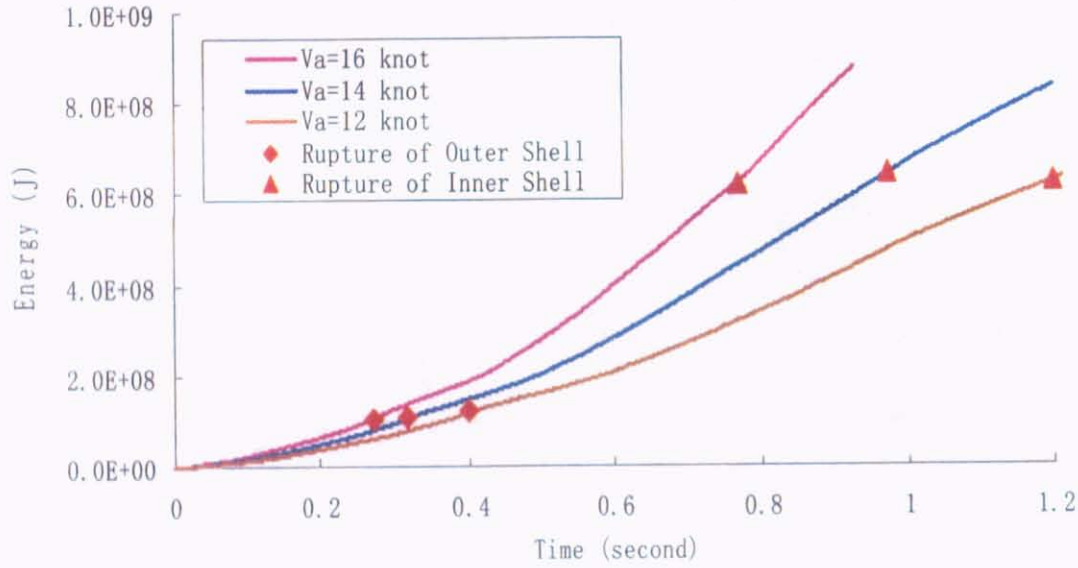

Fig. 7.10 Internal energy-time curve for various initial velocities of striking ship

The effect of striking ship velocity on the obtained impact force-time curves and internal energy-time curves are shown in Fig. 7.9 and 7.10. If we compare with the results at the same collision time, the absorbed internal energy of struck tank and the impact force between the bow and struck area depends strongly on the striking ship velocity. The larger the striking ship velocity, the larger the strain energy and the impact force. Decreasing the collision velocity of the striking ship can effectively avoid the damaged extent of struck tank structures.

In Table 7.3, the penetration depths, impact forces, energy results, motion results and critical striking velocities at the point of inner shell rupture for three different initial velocity of striking ship are given. Figure 7.11 and 7.12 show the impact force-penetration curves and absorbed energy-penetration curves for various initial striking velocities.

Table 7.3 Simulation results at rupture time of the inner side shell for different initial striking velocities

Initial Velocity of Striking Ship(knot)	16	14	12
Time of Inner Shell Rupture(s)	0.768	0.974	1.200
Penetration Depth (m)	5.65	5.95	5.84
The Impact Force (MN)	220	232	218
Kinetic Energy of Striking Ship(MJ)	1660	1015	553
Velocity of Striking Ship(m/s)	5.83	5.31	3.92
Kinetic Energy of Surrounding Water (MJ)	36	25	31
Kinetic Energy of Struck Ship(MJ)	62	92	105
Velocity of Struck Ship(m/s)	0.65	0.79	0.845
Internal Energy of Struck Ship(MJ)	623	643	625
Critical Striking Velocity(m/s)	4.38	4.45	4.39

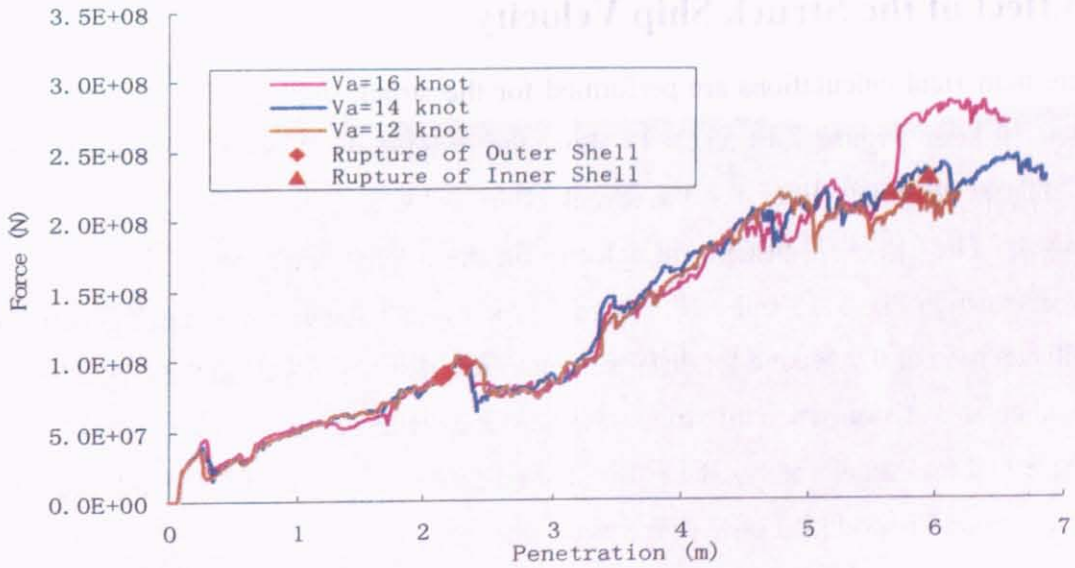

Fig. 7.11 Force-penetration curve for various initial velocity of striking ship

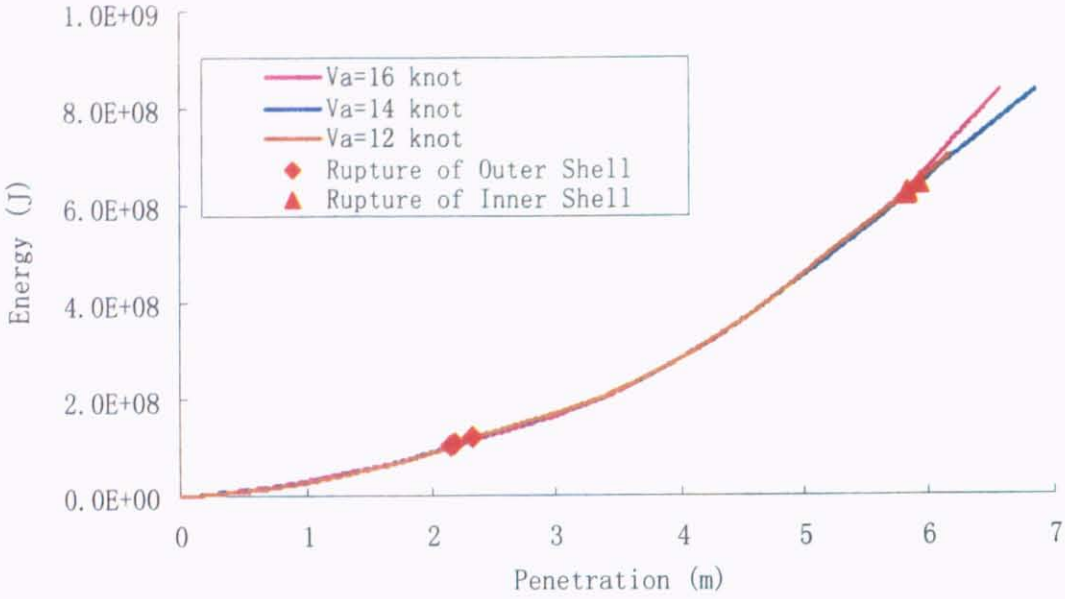

Fig. 7.12 Absorbed energy-penetration curve for various initial velocity of striking ship

It is interesting that the impact force and absorbed internal energy is similar at the time of inner shell rupture for various initial striking velocities. When we derive the critical striking velocity in simplified analytical method, one assumption is that the critical absorbed internal energy is not change with various initial striking velocities. The simulation results show that this assumption is right.

7.4 Effect of the Struck Ship Velocity

Here numerical calculations are performed for the struck ship velocity with 0 knot, 8 knot and 16 knot. Figure 7.13 and 7.14 show the progressive damage process of struck cargo tank at different time for the struck ship velocity with 8 knot and 16 knot, respectively. The effect of struck ship velocity on the impact force and absorbed internal energy is shown in Fig. 7.15 and 7.16. Figure 7.17 shows a comparison of the side damages at a collision time of 0.9 second for different velocities of struck ship. The damage extent of a perpendicular collision when the struck ship was at a standstill was smaller than when the struck ship had forward velocity. The effect of struck ship velocity could lead to less energy absorption capability and also earlier rupture of inner shell.

Rupture of outer shell T=0.168 s

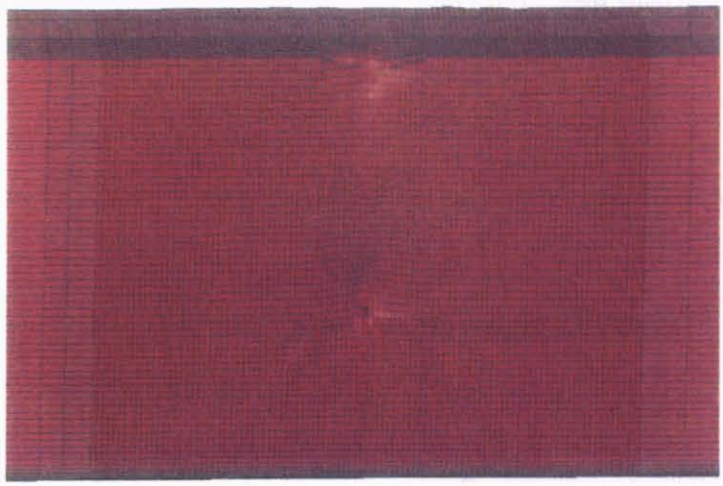

Rupture of inner shell T=0.590 s

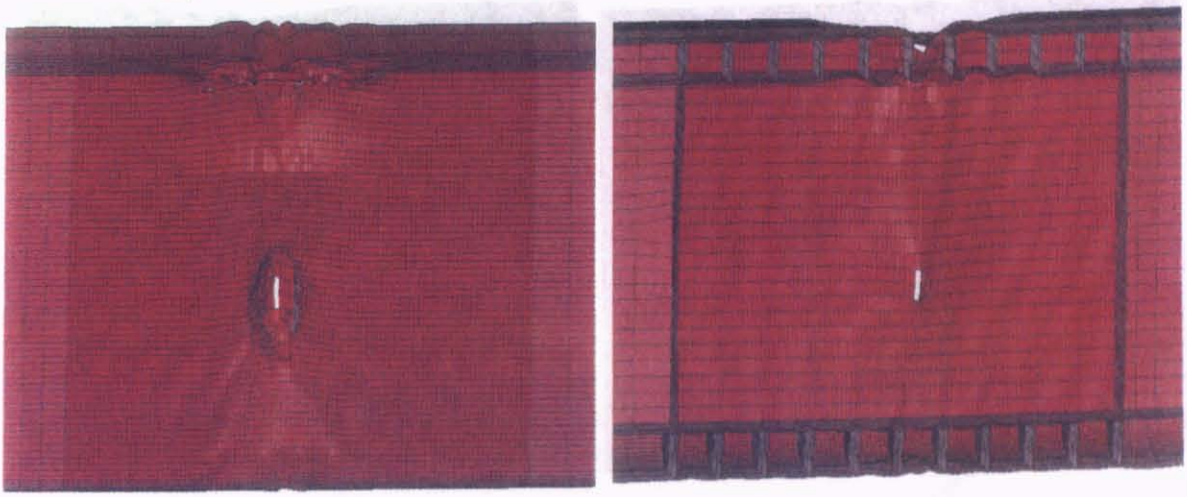

T=1.0 s

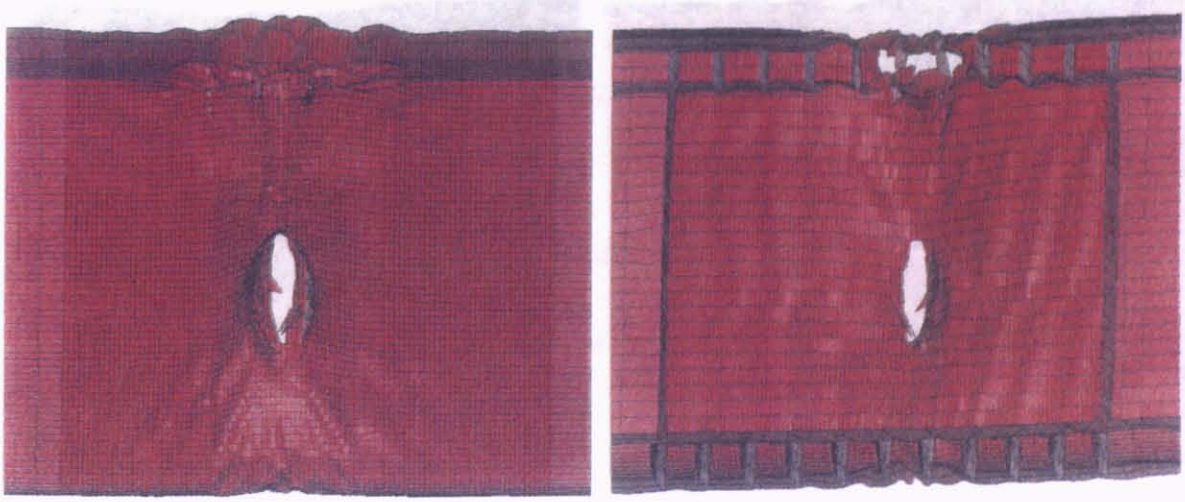

Fig. 7.13 Damaged tank at different time for struck ship velocity 8 knot

Rupture of outer shell T=0.134 s

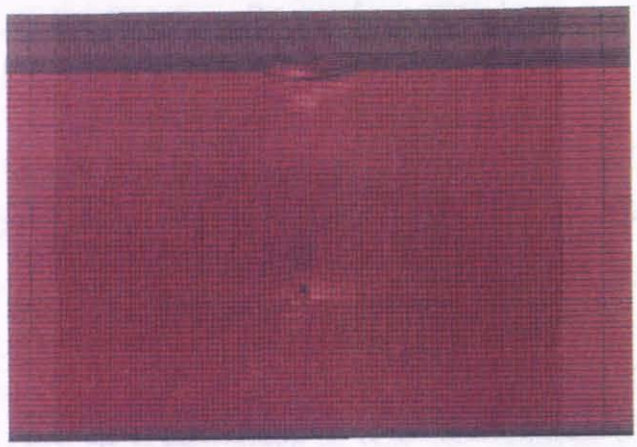

Rupture of inner shell T=0.512 s

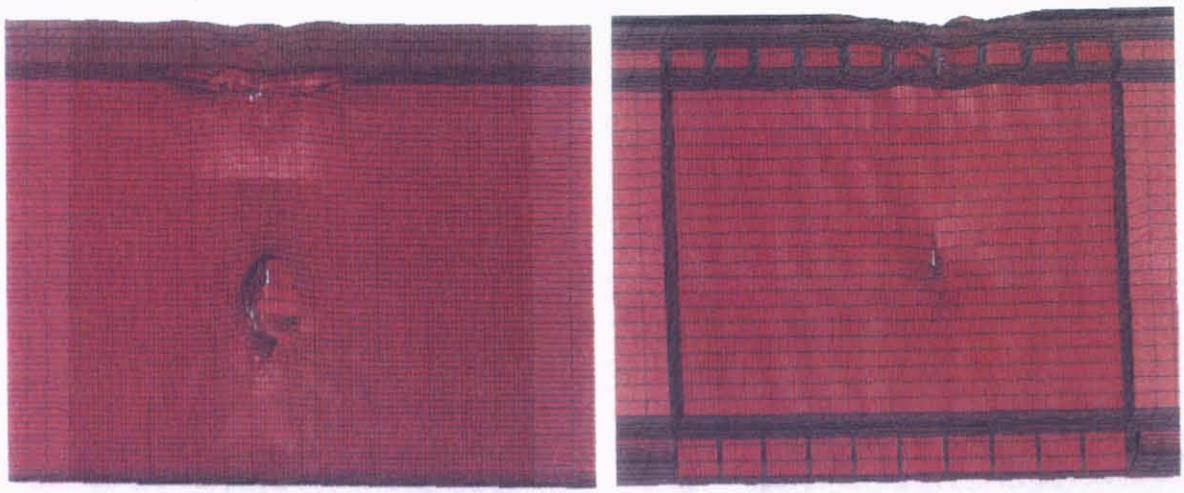

T=1.0 s

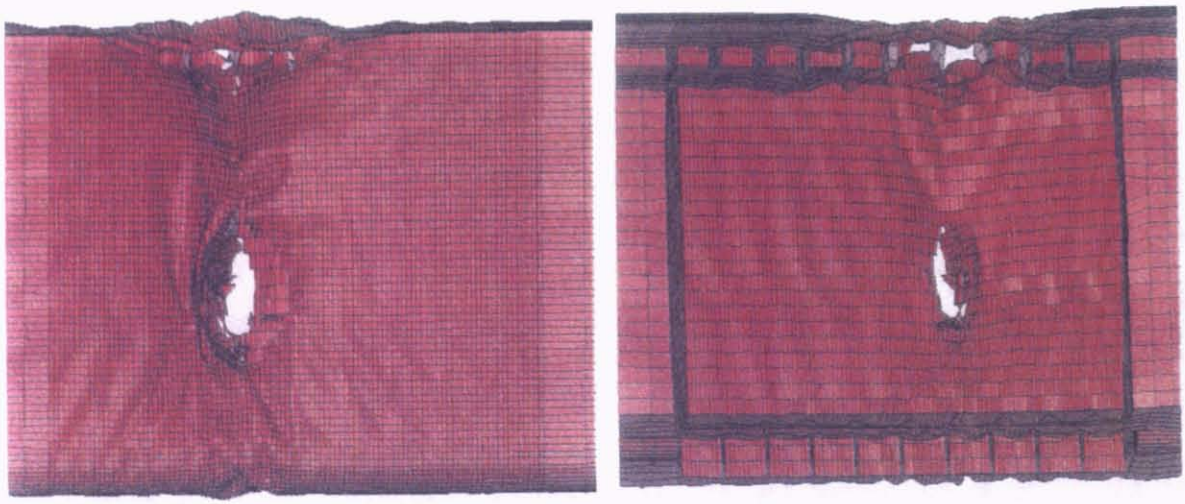

Fig. 7.14 Damaged tank at different time for struck ship velocity 16 knot

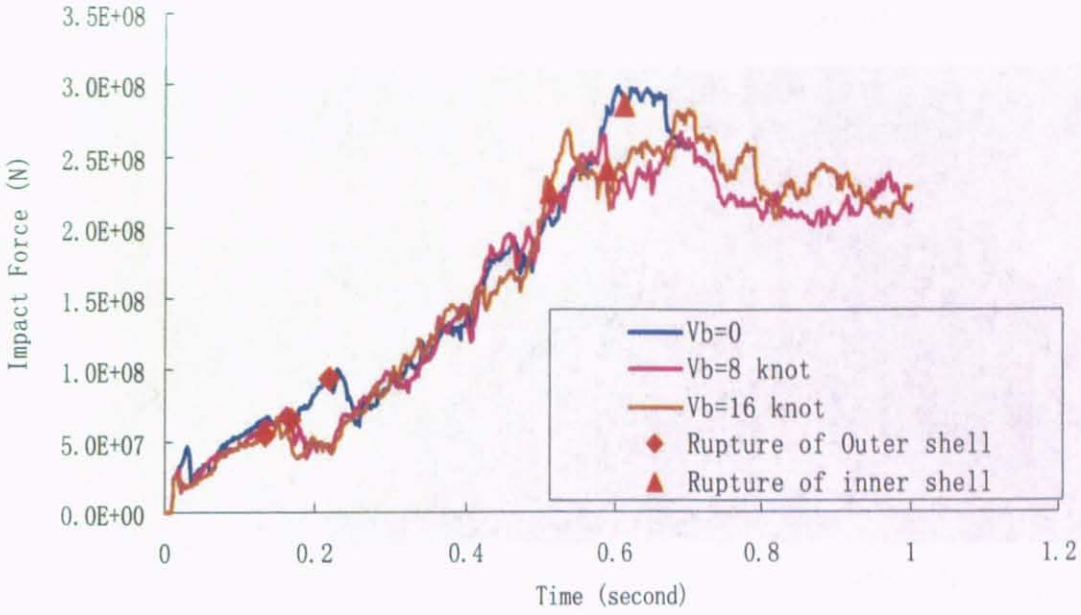

Fig. 7.15 The impact force-time for various velocities of struck ship

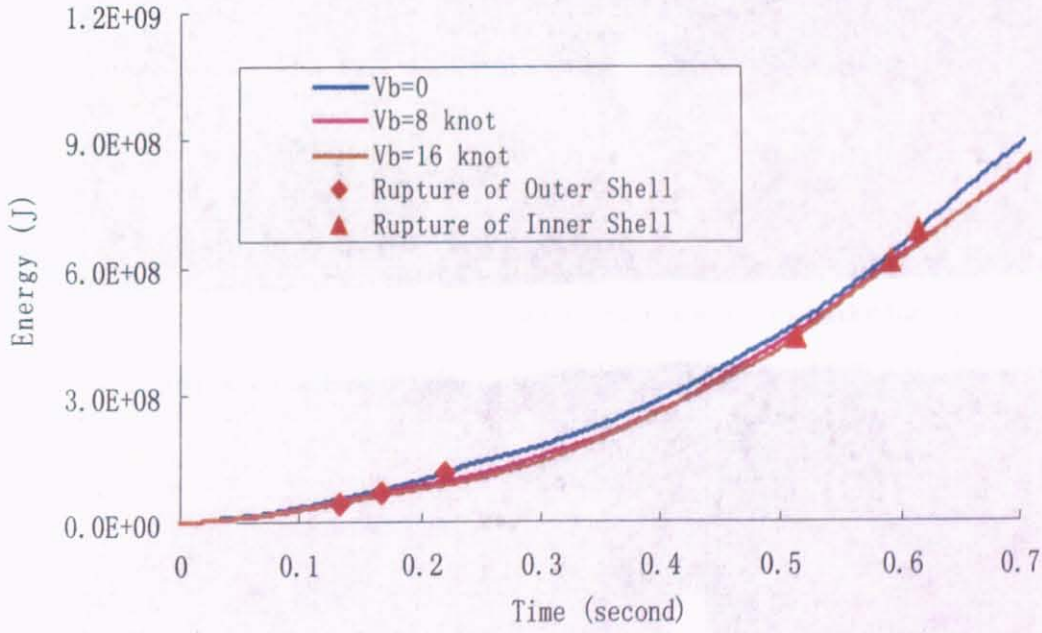

Fig. 7.16 Internal energy-time for various velocities of struck ship

$V_b = 0\,knot$

$V_b = 8\,knot$

$V_b = 16\,knot$

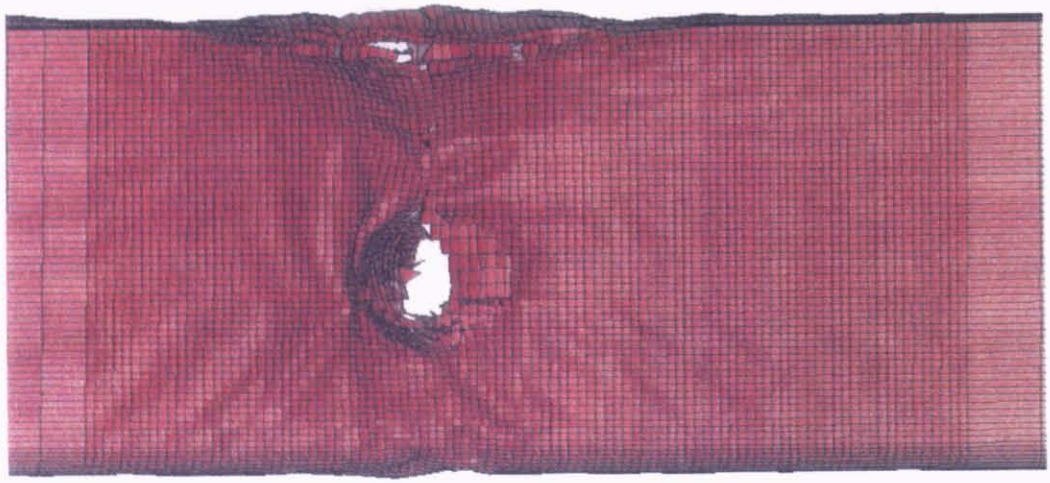

Fig. 7.17 Damages to the side structures at a collision time of 0.9second

In Table 7.4, the penetration depths, impact forces, energy results, motion results at the point of inner shell rupture for three different forward velocities of struck ship are given. Larger the struck ship velocity is, smaller impact force and critical absorbed energy at the point of inner shell rupture are.

Table 7.4 Simulation results at rupture time of the inner side shell for different velocities of struck ship

Velocity of Struck Ship(knot)	0	8	16
Time of Inner Shell Rupture(s)	0.614	0.590	0.512
Penetration Depth (m)	5.77	5.65	4.97
The Impact Force (MN)	287	242	226
Kinetic Energy of Striking Ship(MJ)	1874	1966	2069
Velocity of Striking Ship(m/s)	7.21	7.39	7.57
Kinetic Energy of Surrounding Water (MJ)	8	12	15
Kinetic Energy of Struck Ship(MJ)	60	2337	9268
Velocity of Struck Ship(m/s)	0.64	3.99	7.95
Internal Energy of Struck Ship(MJ)	646	597	496
Critical Striking Velocity(m/s)	4.55	4.32	3.99

7.5 Effect of Collision Angle

During the ship collision statistical accident data, the collision angle is different. In order to investigate effect of collision angle on the rupture of struck liquid cargo tank, numerical simulations are performed for collision angle of $90°$, $75°$ and $60°$. Figure 7.18 and 7.19 shows the impact force and absorbed internal energy curves for different collision angles. In Table 7.4, the penetration depths, impact forces, energy results, motion results at the point of inner shell rupture for three different collision angles are given.

The ultimate load-carrying capacity, which is determined by damaged structural area and the rupture of inner shell, increases with the decrease of collision angle. The rupture of inner shell occurs early for perpendicular collision ($90°$). The load-carrying capacity of side structures depends strongly on the collision angle. In order to evaluate the

crashworthiness of side structure more precisely, effect of collision angle should be taken into account.

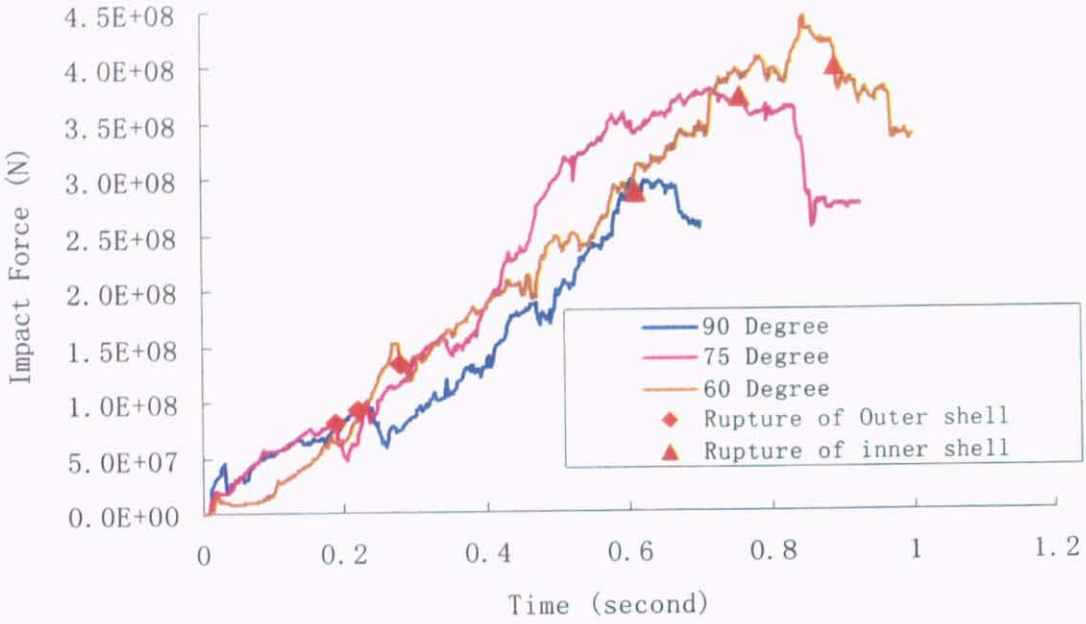

Fig. 7.18 Impact force-time for various collision angles

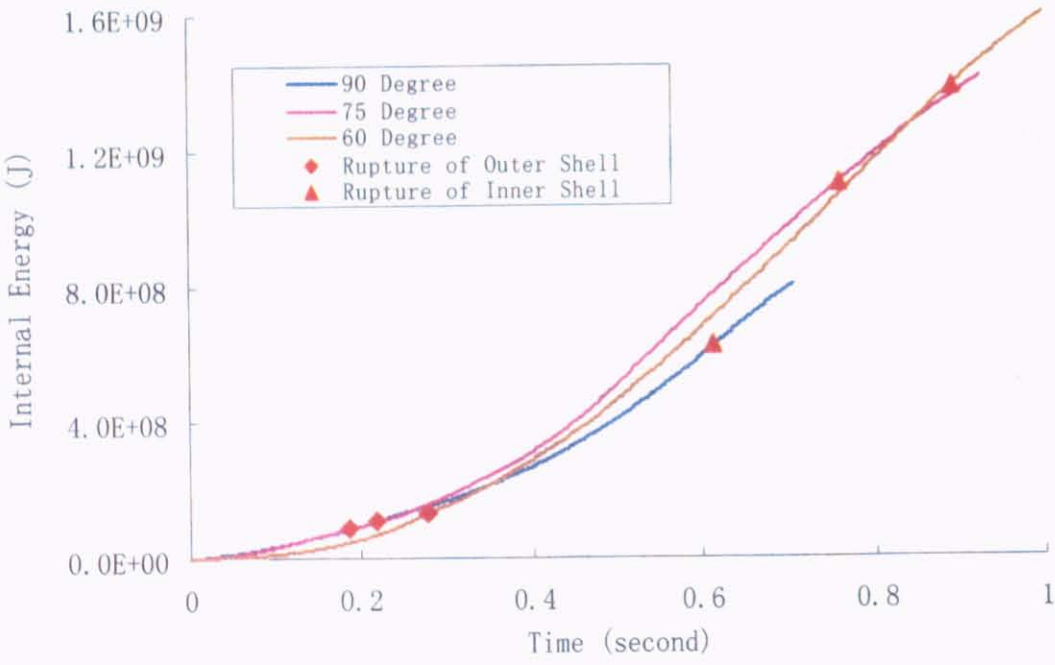

Fig. 7.19 Internal energy force-time for various collision angles

$\theta = 90°$

$\theta = 75°$

$\theta = 60°$

Fig. 7.20 Damages to the side structures at collision time of 0.7 second

Table 7.5 Simulation results at rupture time of the inner side shell for different collision angles

Collision Angle(degree)	90	75	60
Time of Inner Shell Rupture(s)	0.614	0.76	0.892
Penetration Depth (m)	5.83	7.54	7.04
The Impact Force (MN)	287	372	399
Kinetic Energy of Surrounding Water (MJ)	10	11	14
Kinetic Energy of Struck Ship(MJ)	60	181	183
Velocity of Struck Ship(m/s)	0.64	1.11	1.12
Internal Energy of Struck Ship(MJ)	646	1107	1387
Critical Striking Velocity (m/s)	4.55	5.83	6.53

Figure 7.20 shows a comparison of the side damages at a collision time of 0.7 second for different collision angle. If we compare the load-carrying capacity at the same collision time, side collision at 60° results in the least damage extent on side structure.

7.6 Remarks

To understand the structural damage behavior of liquid cargo carrier better, the detailed parameter study was carried out. The effect of the following parameters, i.e. the initial striking ship velocity, struck ship velocity, collision angle and different ship types of the striking ship, is discussed. The effect of initial striking ship velocity is significant to the impact force-time curve and absorbed energy-time curve. However, the critical absorbed internal energy, impact force, penetration depth and critical striking velocity is independent of the initial striking velocity at the time of rupture of inner shell structure. Less energy was dissipated at the point of rupture of the inner side when the struck ship had a forward velocity than when it was at standstill. The damage extent of a perpendicular collision when the struck ship was at a standstill was smaller than when the struck ship had forward velocity. The perpendicular collision (90°) causes the maximum internal energy to side structures at the same collision time. Changing the collision angle can decrease the damage of struck ship. For different loading conditions the impact force as well as the structural

absorbed energy varied with the contact location, the mass of striking ship and size of bow. Based on FEM simulation results, some conclusions and advices are derived as following:

1) To assess the crashworthiness of side structure, relatively large initial striking velocity can be used.
2) The impact force and absorbed internal energy decrease at the point of outer/inner shell rupture as the struck ship velocity increases.
3) The impact force and absorbed energy at the point of outer/inner shell rupture vary with collision angles.
4) For different loading conditions, the crashworthiness of side structure varies with the vertical contact point, the mass of striking ship and size of bow.